Autonomous planning of optimal four-dimensional trajectory for real-time en-route airspace operation with solution space visualisation

实时航路空域操作中四维轨迹的最优自主规划及解空间可视化

Yutong Chen, Minghua Hu, Lei Yang*
陈宇通，胡明华，杨磊 *
Nanjing University of Aeronautics and Astronautics, Nanjing, 210000, China
南京航空航天大学，南京，210000，中国

A R T I C L E I N F O

文章信息

Keywords:
关键词:
Autonomous air traffic operation
自主空中交通操作
Conflict resolution
冲突解决
Trajectory-based operation
基于轨迹的操作
Free route airspace
自由航线空域
Solution space visualisation
解空间可视化

A B S T R A C T

摘要

One of the challenges in applying autonomous operation-based conflict detection and resolution (CD&R) techniques to practice is their functional completeness, such as the ability to simultaneously consider three-dimensional (3D) scenarios, controlled time of arrival, restricted areas, trajectory recovery, and multi-stakeholder performance preferences. Besides, the effective interaction between controllers, pilots and autonomous operating system can better support the CD&R to work in practice, where humans are able to intuitively understand the rationale for solutions given by automatic decision-making tools. To bridge the gap, a novel operational framework for four-dimensional (4D) trajectory conflict management in the context of free route airspace is proposed. Airspace discretisation based on a 3D grid is used to facilitate the consideration of restricted areas and to balance calculation speed and optimal effect. The core of this framework is a two-stage real-time autonomous 4D trajectory planning method in a restricted en-route sector with multiple flight levels enhanced by solution space visualisation. Stage one is a trajectory pre-planning model based on a visibility graph and the Dijkstra algorithm considering the conflict between aircraft and emerging restricted areas. Stage two is a real-time conflict-free and fuel-optimal 4D trajectory re-planning model. The space-time prism is employed to enable the planned trajectory to meet the controlled time of arrival and trajectory recovery requirements, where the performance preferences of both the air traffic management and airspace users are taken into account. The reachable solution space representation is applied to realise the solution space visualisation that has the potential to support the human-machine interaction and air-ground coordination. A simulation scenario is established to validate the effectiveness, efficiency, stability, and timeliness of the proposed method. Results show that in an artificial en-route sector, the average extra flight distance, average flight delay, average extra fuel consumption, and average computing time for conflict resolution were less than 0.41 km , 2.1 s, 1.5 kg , and 0.08 s in the saturated scenario, respectively, and the domino effect of the flight conflict did not show a significant rise with the increase of traffic density, which verified that the proposed autonomous trajectory operation methodology is a promising approach to facilitate autonomous air traffic management in the future.

将自主操作基础的冲突检测与解决 (CD&R) 技术应用于实际操作中的一个挑战是它们的功能完整性，例如同时考虑三维 (3D) 场景、控制到达时间、限制区域、轨迹恢复以及多方性能偏好的能力。此外，控制器、飞行员与自主操作系统之间的有效互动可以更好地支持 CD&R 在实际中的应用，其中人类能够直

观地理解自动决策工具给出的解决方案的理由。为了弥补这一差距，提出了一种新颖的运营框架，用于自由航线空域中四维 (4D) 轨迹冲突管理。基于三维网格的空域离散化被用来考虑限制区域，并平衡计算速度和最优效果。该框架的核心是在受限航路扇区内的多飞行高度上增强的实时自主 4D 轨迹规划的两阶段方法，并通过解决方案空间可视化进行改进。第一阶段是基于可视图和 Dijkstra 算法的轨迹预规划模型，考虑飞机与新兴限制区域之间的冲突。第二阶段是实时无冲突且燃油最优的 4D 轨迹重规划模型。时空棱镜被用来确保规划轨迹满足控制到达时间和轨迹恢复的要求，同时考虑空中交通管理和空域用户的性能偏好。可达解决方案空间表示法被应用于实现解决方案空间可视化，这有可能支持人机交互和空地协调。建立了一个模拟场景来验证所提出方法的有效性、效率、稳定性和及时性。结果显示，在人工航路扇区中，冲突解决的额外飞行距离平均值、平均飞行延误、平均额外燃油消耗和平均计算时间分别小于 0.41 km 、2.1 s, 1.5 kg 和 0.08 s ，在饱和场景下，航班冲突的连锁反应并没有随着交通密度的增加而显著上升，这验证了所提出的自主轨迹操作方法学是未来促进自主空中交通管理的一个有前景的方法。

1. Introduction

1. 引言

At present, air traffic is in a stage of rapid development. Global air traffic has doubled in size once every 15 years since 1977 and will likely continue to do so (ICAO, 2013). Although the COVID-19 has led to a decline in air traffic worldwide from 2020, it is only temporary (Zhu et al., 2021). In the long run, air traffic will continue to grow. Subsequently, the contradiction between air traffic demand and capacity is becoming increasingly prominent, which is mainly manifested in the increase in flight delays and cancellations. In Europe, for example, flight delays averaged 13.1 min in2019, up 13.7% from 2016. In addition, the number of flights with delays longer than 30 min increased to 12.1% , and an average of 1.7% of flights were cancelled each month (EUROCONTROL, 2020; Xu et al., 2020). Therefore, it is urgent to improve air traffic management (ATM) capacity.

目前，航空交通正处于快速发展阶段。自 1977 年以来，全球航空交通每 15 年翻一番，未来可能还会继续这样增长 (国际民航组织，2013 年)。尽管自 2020 年以来，COVID-19 导致了全球航空交通的下降 (朱等人，2021 年)，但这只是暂时的。从长远来看，航空交通将继续增长。因此，航空交通需求与容量之间的矛盾日益突出，主要表现在航班延误和取消数量的增加。例如，在欧洲，2019 年的航班延误平均为 13.1 min ，比 2016 年增加了 13.7% 。此外，延误超过 30 min 分钟的航班数量增加到 12.1% ，每月平均有 1.7% 的航班被取消 (EUROCONTROL，2020 年；徐等人，2020 年)。因此，迫切需要提高航空交通管理 (ATM) 的能力。

The workload of air traffic controllers is considered to be one of the critical constraints on the growth of air traffic (Velasco et al., 2010). There is a direct correlation between a controller's workload and the traffic volume (Djokic et al., 2010). To break through this bottleneck, Artificial Intelligence algorithms and decision support tools have been developed and applied in air traffic control practice. The purpose is to assist the controllers in completing conflict resolution (CR), thus reducing the controller's workload. For this issue, centralised control is mainstream. The advantage of centralised control is that it can obtain the global optimal solution based on global information. At first, some CR models were established mainly using linear programming methods and optimisation control theory (Xu et al., 2020; Alonso-Ayuso et al., 2010). On this basis, the introduction of the concept of priority enables aircraft involved in multi-aircraft conflict groups to be freed according to the priority sequence. Subsequently, artificial intelligence algorithms such as the genetic algorithm were gradually applied for CR (Hu et al., 2004; Alonso-Ayuso et al., 2016), and the effects of integrated algorithms composed of multiple intelligent algorithms were proven to be better than those of single algorithms (Alam et al., 2009; Wang et al., 2020). Several experiments have proven that the effect of multi-phase planning or stepwise disengagement on CR is better than that of one-time disengagement (Cecen and Cetek, 2019; Walter and Kostina, 2014). In addition, discretisation of space can greatly reduce the complexity of a conflict model, thus effectively improving the computing speed (Omer, 2015). In addition to supporting the decision-making function of normal operating conditions, CR in contingent situations, e.g., emerging restricted airspace, has gradually attracted the attention of researchers (Kreuz et al., 2016).

空管人员的工负荷被认为是限制航空交通增长的关键约束之一 (Velasco 等人，2010 年)。管制员的工负荷与交通量之间存在直接相关性 (Djokic 等人，2010 年)。为了突破这一瓶颈，已经开发并将人工智能算法和决策支持工具应用于空中交通管制实践中。其目的是协助管制员完成冲突解决 (CR)，从而减轻管制员的工负荷。对于这一问题，集中控制是主流。集中控制的优点在于可以根据全局信息获得全局最优解。

* Corresponding author.
* 通讯作者。
E-mail addresses: chenyutong@nuaa.edu.cn (Y. Chen), minghuahu@nuaa.edu.cn (M. Hu), laneyoung@nuaa.edu.cn (L. Yang).
电子邮件地址:chenyutong@nuaa.edu.cn (Y. 陈), minghuahu@nuaa.edu.cn (M. 胡), laneyoung@nuaa.edu.cn (L. 杨)。

最初，一些 CR 模型主要是使用线性规划方法和优化控制理论建立的 (Xu 等人，2020 年；Alonso-Ayuso 等人，2010 年)。在此基础上，引入优先级概念使得涉及多机冲突组的飞机能够根据优先顺序释放。随后，遗传算法等人工智能算法逐渐应用于 CR(Hu 等人，2004 年；Alonso-Ayuso 等人，2016 年)，并且证明了由多种智能算法组成的集成算法的效果要优于单一算法 (Alam 等人，2009 年；Wang 等人，2020 年)。多项实验证明，多阶段规划或逐步解除对 CR 的效果要优于一次性解除 (Cecen 和 Cetek，2019 年；Walter 和 Kostina，2014 年)。此外，空间的离散化可以大大降低冲突模型的复杂性，从而有效提高计算速度 (Omer, 2015 年)。除了支持正常运营条件下的决策功能外，应急情况下的 CR，例如出现的限制空域，也逐渐引起了研究者的关注 (Kreuz 等人，2016 年)。

To further improve the ATM capacity, the concept of free flight was proposed, which is committed to transferring part of the separation assurance function from the ground to the air, that is, from controllers to pilots (Ruigrok and Hoekstra, 2007; Kahne, 2000). If free flight is applied in practice, it will change the ATM system significantly, from centralised control to distributed operation (Hoekstra et al., 2002). In contrast to centralised control, distributed control has the advantage of lower computational costs, but the disadvantage is that it cannot guarantee that the global optimal solution will be found. Hybrid system dynamics promote the development of distributed control in ATM (Pappas et al., 1997), and distributed artificial intelligence takes distributed control to the next level (Blom and Bakker, 2016). Experiments showed that distributed control has stronger robustness and fewer conflicts in airspace with high traffic density (Hoekstra et al., 2001). The uncertain factors were incorporated into the study of distributed control, such as navigation accuracy and human factors (Marshall et al., 2017). The cellular automata method based on space discretisation brought convenience to the conflict solution (Shijin et al., 2017).

为了进一步提高空中交通管理 (ATM) 能力，提出了自由飞行的概念，该概念致力于将部分分离保障功能从地面转移到空中，即从管制员转移到飞行员 (Ruigrok 和 Hoekstra，2007；Kahne，2000)。如果在实际中应用自由飞行，它将显著改变 ATM 系统，从集中控制转变为分布式操作 (Hoekstra 等人，2002)。与集中控制相比，分布式控制的优势在于计算成本较低，但缺点是它无法保证找到全局最优解。混合系统动力学促进了分布式控制在 ATM 中的发展 (Pappas 等人，1997)，分布式人工智能将分布式控制提升到了一个新的水平 (Blom 和 Bakker，2016)。实验表明，在交通密度高的空域中，分布式控制具有更强的鲁棒性和更少的冲突 (Hoekstra 等人，2001)。不确定性因素被纳入分布式控制的研究中，例如导航精度和人为因素 (Marshall 等人，2017)。基于空间离散化的细胞自动机方法为解决冲突带来了便利 (Shijin 等人，2017)。

However, the improvement of the airspace performance by either supporting decision-making tools based on centralised control or free flight based on distributed control seems insignificant. On one hand, the long calculation time of the global optimisation algorithm makes the centralised control method almost impossible to be used in high-density airspace in real-time operation (that is, the tactical phase). On the other hand, for free flight, it is difficult for the crew to complete conflict detection and resolution (CD&R) independently (Alam et al., 2009), especially when the pilot continues to operate the aircraft (Hoekstra et al., 2002). Therefore, to increase air traffic from the perspective of reducing the workload of controllers, it seems a more promising development direction is needed to delegate the task of CD&R to automated systems, namely, autonomous operation (Idris et al., 2016).

然而，无论是通过基于集中控制的决策支持工具还是基于分布式控制的自由飞行来提升空域性能，其效果似乎都不显著。一方面，全局优化算法的长计算时间使得集中控制方法几乎无法在实时运行 (即战术阶段) 的高密度空域中使用。另一方面，对于自由飞行，机组人员独立完成冲突检测与解决 (CD&R) 是困难的 (Alam 等人，2009 年)，尤其是在飞行员继续操纵飞机的情况下 (Hoekstra 等人，2002 年)。因此，从减轻管制员工作负荷的角度来增加空中交通量，似乎需要更有前景的发展方向，即将 CD&R 的任务委托给自动化系统，即自主运行 (Idris 等人，2016 年)。

The concept of trajectory-based operation (TBO) (ICAO, 2005) is moving the autonomous operation one step closer to practical use. TBO is a new ATM paradigm in which every aircraft is represented by a four-dimensional (4D) trajectory. A 4D trajectory includes a series of points from departure to arrival representing the aircraft's path in four dimensions: lateral (latitude and longitude), vertical (altitude), and time (Gardi et al., 2015). Controlled time of arrival (CTA), considered as one of the fundamental features of TBO (Sun et al., 2019), is an ATM-imposed time constraint on a defined point along the flight path to be achieved within a required accuracy using feedback control, which greatly reduces the uncertainty of flight operations (Weitz et al., 2019). In this context, artificial intelligence-based CR algorithms have been better applied. For example, a recent study proposed a stochastic linear hybrid system to describe the dynamics of an aircraft with changing flight modes, and a computationally efficient algorithm was developed to estimate aircraft future trajectories (Seah and Hwang, 2009). A method of obtaining a conflict-free solution for all planned trajectories during the strategic phase was presented, which was based on a data-driven CR model and a multi-objective global optimisation algorithm (Calvo-Fernández et al., 2017). It was found out that time-based waypoints alone can guarantee conflict-free trajectories if certain initial conditions are satisfied (Sun et al., 2019). Moreover, when a hazardous weather area is to be modelled, it is considered to be a moving object that is included in the optimisation model, which better avoids the conflict between aircraft and dangerous weather (Seenivasan et al., 2020).

基于轨迹的操作 (TBO) 概念 (ICAO，2005 年) 使自主操作向实际应用迈进了一步。TBO 是一种新的空

中交通管理 (ATM) 范式，其中每架飞机都由一个四维 (4D) 轨迹表示。4D 轨迹包括从起飞到降落的一系列点，代表飞机在四个维度上的路径: 水平 (纬度和经度)、垂直 (高度) 和时间 (Gardi 等人，2015 年)。受控到达时间 (CTA)，被视为 TBO 的基本特征之一 (Sun 等人，2019 年)，是 ATM 对飞行路径上定义的点施加的时间约束，要求在所需的精度内使用反馈控制来实现，这大大降低了飞行操作的不确定性 (Weitz 等人，2019 年)。在这种情况下，基于人工智能的冲突解析 (CR) 算法得到了更好的应用。例如，最近的一项研究提出了一种随机线性混合系统来描述飞机在改变飞行模式时的动力学，并开发了一种计算效率高的算法来估计飞机未来的轨迹 (Seah 和 Hwang，2009 年)。提出了一种在战略阶段为所有计划轨迹获得无冲突解决方案的方法，该方法基于数据驱动的 CR 模型和多目标全局优化算法 (Calvo-Fernández 等人，2017 年)。研究发现，如果满足某些初始条件，仅基于时间的航点 alone 可以保证轨迹无冲突 (Sun 等人，2019 年)。此外，当需要模拟危险天气区域时，将其视为一个移动对象，包括在优化模型中，这更好地避免了飞机与危险天气之间的冲突 (Seenivasan 等人，2020 年)。

The emergence of free route airspace (FRA) has further enabled autonomous operation. FRA is the specified airspace within which users may freely plan a route between a defined entry point and a defined exit point, with the possibility to route via intermediate waypoints, without reference to the air traffic service route network, subject to airspace availability (Rezo and Steiner, 2020; Gaxiola et al., 2018). FRA expands the operating space of aircraft from air routes to the entire airspace. In this context, due to the expansion of spatial dimensions, grid-based discretisation methods are widely used to transform the space from continuous to discrete, which brings convenience for optimisation (Coletsos and Ntakolia, 2017; Drupka et al., 2018).

自由航线空域 (FRA) 的出现进一步促进了自主运行。FRA 是指用户可以在其中自由规划从定义的入口点至定义的出口点之间的航路，并且可以经过中间航点，无需参照空中交通服务航线网络，但受空域可用性的限制 (Rezo 和 Steiner，2020；Gaxiola 等人，2018)。FRA 将飞机的运行空间从航线扩展到整个空域。在此背景下，由于空间维度的扩展，基于网格的离散化方法被广泛用于将空间从连续转换为离散，这为优化带来了便利 (Coletsos 和 Ntakolia，2017；Drupka 等人，2018)。

The interaction of controllers, pilots and machine is an important issue that should be considered in autonomous ATM research. Human involvement in autonomous ATM is necessary (at least in the initial stage), because ATM is a life-critical system. The application of autonomous operation systems to practice presupposes mutual trust between the various parties involved, mainly controllers, pilots and machines. Understanding is the basis of trust. In an autonomous operating environment, it would be detrimental if controllers, pilots, and automated programs did not understand each other's intentions. Adequate understanding and trust ensure controllers and pilots can effectively monitor and take control of automated equipment at any time. One of the key issues of system design for human-machine collaboration is that operations must be capable of being safely taken over by humans under any circumstances. Therefore, the internal logic of the machine must be transparent and understandable, and the cognition of humans and machines needs to be strongly synchronised (Saez Nieto, 2016). The controller's situational cognition of automation equipment has an important influence on the controller's workload (Edwards et al., 2017). In autonomous ATM, efficient human-machine interaction can be described as one in which (a) the machine can make decisions based on human preferences (e.g. performance preferences of multiple stakeholders) and (b) the human can intuitively understand the machine's decisions (e.g. the reasons for a decision made by the machine and the foreseeable consequences). The transparency of autonomous operating systems has been proven to be effective in CR (Westin et al., 2016). Scholars have tried to build a set of CR models by exploring and summarising the methods of CR for controllers in actual operation (Eyferth et al., 2003; Karikawa and Aoyama, 2016). Through the research and application of the visualised decision support tools, it was found that the visualised interface of CD&R based on graphics could effectively enhance the understandability of decision support tools (Velasco et al., 2010; Strybel et al., 2016). Since visualisation of the airspace situation can enhance the comprehensibility of the intentions of both air and ground (pilots and controllers), it can facilitate air-ground coordination, while air-ground coordination is an effective way to improve operational safety (Lai et al., 2019). If controllers and pilots could visualise all feasible trajectories and their corresponding costs on a human-machine interface (i.e., solution space visualisation), this would undoubtedly help humans understand the machine's decisions. For CD&R research, the solution space visualisation can be a potential method to support visualisation-based human-machine interaction.

控制员、飞行员与机器的交互是一个在自主空中交通管理 (ATM) 研究中应当考虑的重要问题。在自主 ATM 中，人类的参与是必要的 (至少在初始阶段)，因为 ATM 是一个与生命安全相关的系统。将自主操作系统应用于实践的前提是参与各方之间相互信任，主要是控制员、飞行员和机器之间。理解是信任的基础。在自主操作环境中，如果控制员、飞行员和自动化程序不能理解彼此的意图，那将是弊大于利的。足够理解和信任确保控制员和飞行员能够在任何时候有效地监控并接管自动化设备。人机协作系统设计的关键问题之一是，操作必须能够在任何情况下安全地由人类接管。因此，机器的内部逻辑必须是透明且可理解的，人类与机器的认知需要紧密同步 (Saez Nieto, 2016)。控制员对自动化设备的情境认知对控制员的工作负荷有重要影响 (Edwards et al., 2017)。在自主 ATM 中，高效的人机交互可以描述为:(a) 机器能够根据人类的偏好 (例如，多个利益相关者的性能偏好) 做出决策；(b) 人类能够直观地理解机器的决策 (例如，机器做出决策的原因和可预见的后果)。自主操作系统的透明性在 CR 中已被证明是有效的 (Westin et al.,

2016)。学者们试图通过探索和总结实际操作中控制员的 CR 方法来构建一套 CR 模型 (Eyferth et al., 2003; Karikawa 和 Aoyama, 2016)。通过可视化决策支持工具的研究与应用，发现基于图形的 CD&R 可视化界面能够有效提高决策支持工具的可理解性 (Velasco et al., 2010; Strybel et al., 2016)。由于对空域情况的可视化能够提高空中和地面 (飞行员和控制员) 意图的可理解性，它能够促进空地协调，而空地协调是提高操作安全的有效途径 (Lai et al., 2019)。如果控制员和飞行员能够在人机界面上可视化所有可行的轨迹及其相应的成本 (即解决方案空间可视化)，这无疑将帮助人类理解机器的决策。对于 CD&R 研究，解决方案空间可视化可以成为支持基于可视化的好人机交互的潜在方法。

Table 1

表 1

Features of real-time CD&R technologies applied to 3D scenarios.

实时 CD&R 技术在 3D 场景中的应用特性。

	No. Papers	CTA	Restricted area	Trajectory recovery	Multi- stakeholder performance preferences	Solution- space visualisation	Large- scale scenario	Models	Control	Computing time
	1 Šišlák et al. (2010)	◦	◦	✓		◦	◦	Agent	D	10 s/a
	2 Cobano et al. (2013)	✓	◦	✓		◦	◦	MINLP	C	47 s/5a
3	Alonso-Ayuso et al. (2016)	◦	◦	◦	◦	◦	◦	SMILO	C	35 s/22 a
4	Alonso-Ayuso et al. (2017)	◦	◦	◦	◦	◦	◦	MINLP	C	2 s/4a
5	Pritchett and Genton (2017)	◦	◦	◦	◦	◦	✓	Expert	D	300 s/2 a
6	Wang et al. (2020)	◦	◦	✓		◦	◦	ILP	C	360 s/59 a
7	Han et al. (2019)	✓	✓	✓		◦	◦	SDP	C	9 s/4 a
8	Malaek and Golchoubian (2020)	◦	◦	✓	◦	◦	✓	Expert	C	153 s/7 a
9	Dong et al. (2022)	◦	◦	◦	◦	◦	✓	MARL	D	0.01 s/a
10	This paper	✓	✓	✓	✓	✓	✓	DP+NLIP	D	0.1 s/a

	论文编号	CTA(消费者技术协会)	限制区域	轨迹恢复	多利益相关者性能偏好	解空间可视化	大规模场景	模型	控制	计算时间
	1 Šišlák 等人 (2010)	◦	◦	✓		◦	◦	代理	D	10 s/a
	2 Cobano 等人 (2013)	✓	◦	✓		◦	◦	MINLP(混合整数非线性规划)	C	47 s/5a
3	Alonso-Ayuso 等人 (2016)	◦	◦	◦	◦	◦	◦	SMILO(一种模型集成和分解优化框架)	C	35 秒/22 个 a
4	Alonso-Ayuso 等人 (2017)	◦	◦	◦	◦	◦	◦	MINLP(混合整数非线性规划)	C	2 s/4a
5	Pritchett 和 Genton(2017)	◦	◦	◦	◦	◦	✓	专家	D	300 秒/2 次
6	王等人 (2020)	◦	◦	✓		◦	◦	ILP(整数线性规划)	C	360 秒/59 次
7	韩等人 (2019)	✓	✓	✓		◦	◦	SDP(半定规划)	C	9 秒/4 次
8	Malaek 和 Golchoubian (2020)	◦	◦	✓	◦	◦	✓	专家	C	153 秒/7 次
9	董等人 (2022)	◦	◦	◦	◦	◦	✓	多智能体强化学习 (MARL)	D	0.01 秒/行动 (s/a)
10	本文	✓	✓	✓	✓	✓	✓	DP+NLIP	D	0.1 秒/行动 (s/a)

Based on the above discussion, we believe that a real-time CD&R method for practical applications should integrally consider the features of the controlled time of arrival, restricted areas, trajectory recovery, multi-stakeholder performance preferences, solution space visualisation, computation time, etc. To further illustrate the current development of this field and highlight the gap, several representative multi-aircraft CD&R technologies for real-time en-route airspace operation that can be applied to 3D scenarios are summarised in Table 1 (where the checkmark (✓) means the method has the corresponding feature and the circle mark (◇) means not; large-scale scenario means whether the effectiveness of the method is validated in a large-scale scenario, rather than a toy case with just a few aircraft; C and D of control refer to centralised and decentralised respectively; for the computing time feature, 's' and 'a' refer to second and aircraft respectively). Sislak proposed an agent-based cooperative decentralised CR method which considers the 4D trajectory (Šišlák et al., 2010). Cobano presented a real-time stochastic CD&R system that formulates mixed-integer non-linear programming (MINLP) and employs particle swarm optimisation (PSO) to solve it (Cobano et al., 2013). Ayuso provided a sequential mixed-integer linear optimisation (SMILO) approach for multi-objective CR optimisation to increase the speed of computing (Alonso-Ayuso et al., 2016). And, Ayuso employed variable neighbourhood search (VNS) to tackle the CR problem with the form of MINLP (Alonso-Ayuso et al., 2017). Pritchett proposed a decentralised, negotiated technique for resolving aircraft conflicts, using an expert system based on a sequential bargaining procedure (Pritchett and Genton, 2017). Wang introduced a generic framework for the cooperation of optimisation algorithms where the CR based on a linear integer programming (LIP) model is efficiently solved by a hybrid optimisation method (Wang et al., 2020). Han presented a method for optimal conflict-free aircraft trajectory generation using stochastic dynamic programming (SDP) (Han et al., 2019). Malaek provided a comprehensive algorithm for potential en-route conflict resolutions based on a customised expert system (Malaek and Golchoubian, 2020). Sui used multi-agent reinforcement learning (MARL) techniques to solve the CD&R problem, which considerably improved calculation performance. However, because MARL application in this field is still in the exploratory stage, Sui's method's resolution success rate is only about 60% (Dong et al.,2022). In summary, the existing multi-aircraft CD&R methods for real-time en-route airspace operation cannot fully consider CTA constraints, restricted areas, trajectory recovery, and multi-stakeholder performance preferences in 3D scenarios. On this basis, the methods to consider the solution space visualisation are rarely reported. Thus, from a practical application point of view, current real-time autonomous 4D trajectory planning methods are deficient in terms of both functional completeness and practicality.

基于上述讨论，我们认为实时 CD&R 方法在实际应用中应整体考虑控制到达时间、限制区域、轨迹恢复、多方性能偏好、解空间可视化、计算时间等特征。为了进一步阐述该领域的当前发展并突出差距，本文总结了表 1 中几种代表性的多机 CD&R 技术，这些技术可应用于实时航路空域操作中的 3D 场景 (其中，勾选标记 (✓) 表示方法具有相应特征，圆圈标记 (◇) 表示没有；大规模场景指的是方法的有效性是否在大规模场景中得到验证，而不仅仅是只有几架飞机的玩具案例；控制中的 C 和 D 分别指集中式和分布式；对于计算时间特征，'s' 和'a' 分别指秒和飞机)。Sislak 提出了一种基于代理的协作分布式 CR 方法，该方

法考虑了 4D 轨迹 (Šišlák et al.，2010)。Cobano 展示了一个实时随机 CD&R 系统，该系统构建了混合整数非线性规划 (MINLP) 模型，并采用粒子群优化 (PSO) 方法求解 (Cobano et al.，2013)。Ayuso 提出了一种顺序混合整数线性优化 (SMILO) 方法，用于多目标 CR 优化以提高计算速度 (Alonso-Ayuso et al.，2016)。此外，Ayuso 采用变量邻域搜索 (VNS) 解决形式为 MINLP 的 CR 问题 (Alonso-Ayuso et al.，2017)。Pritchett 提出了一种用于解决飞机冲突的分布式谈判技术，该技术使用基于顺序谈判过程的专家系统 (Pritchett 和 Genton，2017)。Wang 引入了一种优化算法合作的通用框架，其中基于线性整数规划 (LIP) 模型的 CR 通过混合优化方法高效求解 (Wang et al.，2020)。Han 提出了一种使用随机动态规划 (SDP) 生成无冲突最优飞机轨迹的方法 (Han et al.，2019)。Malaek 提供了一个基于定制专家系统的潜在航路冲突解决的综合算法 (Malaek 和 Golchoubian，2020)。Sui 使用多代理强化学习 (MARL) 技术解决 CD&R 问题，显著提高了计算性能。然而，由于 MARL 在此领域的应用仍处于探索阶段，Sui 的方法的解决成功率仅为 60% (Dong et al.，2022)。总之，现有的实时航路空域操作多机 CD&R 方法在 3D 场景中不能完全考虑 CTA 约束、限制区域、轨迹恢复和多方性能偏好。在此基础上，考虑解空间可视化的方法很少被报道。因此，从实际应用的角度来看，当前的实时自主 4D 轨迹规划方法在功能完整性和实用性方面存在不足。

To bridge this gap, we propose an autonomous planning method of optimal 4D trajectory for real-time en-route airspace operation with solution visualisation (the features are also summarised in Table 1). In this method, a general framework of autonomous trajectory operating system with the participation of Airspace Users (AUs) and the ATM is proposed. A two-stage real-time 4D trajectory planning method is designed to accommodate the current trajectory-based operation mechanism. We model the airspace based on discrete 3D grids to facilitate the consideration of restricted areas. The space-time prism method is employed to meet the controlled time of arrival and trajectory recovery requirements and it is enhanced to work with 3D scenarios. Multi-stakeholder performance preferences are considered, such as punctuality, fuel cost, orderliness and safety. An adaptive postponing CTA mechanism is designed to close the loop of conflict resolution. We design a reachable solution space representation to realise the solution space visualisation that facilitates showing all feasible rerouting options and their corresponding costs on the human-machine interface in real-time. The main contributions of this study can be summarised as follows:

为了弥补这一空白，我们提出了一种自主规划方法，用于实时航路空域操作的最优 4D 轨迹，并具备解决方案可视化 (特点也在表 1 中进行了总结)。在此方法中，提出了一个包含空域用户 (AUs) 和空中交通管理 (ATM) 参与的自主轨迹操作系统的一般框架。设计了一个两阶段的实时 4D 轨迹规划方法，以适应当前的基于轨迹的运行机制。我们基于离散的 3D 网格来建模空域，以便考虑限制区域。采用时空棱柱法以满足控制到达时间和轨迹恢复要求，并对其进行增强以适应 3D 场景。考虑了多方利益相关者的性能偏好，如准时性、燃油成本、有序性和安全性。设计了一种自适应延迟 CTA 机制，以实现冲突解决的闭环。我们设计了一种可达解决方案空间表示法，以实现解决方案空间的可视化，便于在实时的人机界面上显示所有可行的改航选项及其相应的成本。本研究的主要贡献可以概括如下:

1. A real-time autonomous 4D trajectory planning method is proposed that is more fully functional than existing methods. This method takes into account not only the manoeuvre of the aircraft in terms of speed, heading and altitude, but also the controlled time of arrival, restricted areas, trajectory recovery and multi-stakeholder performance preferences for practical applications.

1. 提出了一种实时自主 4D 轨迹规划方法，该方法比现有方法的功能更全面。该方法不仅考虑了飞机在速度、航向和高度方面的机动，还考虑了控制到达时间、限制区域、轨迹恢复以及多方利益相关者的性能偏好，以适应实际应用。

2. A framework of autonomous trajectory operation system is designed to be compatible with the current trajectory-based operation mechanism. The real-time autonomous 4D trajectory planning method is divided into two stages, which are used for the generation of the desired trajectory and the agreed trajectory, respectively, in a more optimal manner.

2. 设计了一个与当前基于轨迹的运行机制兼容的自主轨迹操作系统框架。实时自主 4D 轨迹规划方法分为两个阶段，分别用于生成期望轨迹和协商轨迹，以更优的方式分别进行。

3. The proposed method is enhanced by plotting all feasible rerouting options and their corresponding costs on the human-machine interface in real-time without any additional computational cost. The solution space visualisation provides a reference pathway for improving human-machine interaction in autonomous operations.

3. 提出的方法通过在人与机界面实时绘制所有可行的重路由选项及其相应成本，而不产生任何额外的计算成本来增强。解决方案空间的可视化为人机交互在自主操作中的改进提供了参考路径。

4. The performance parameters of the method in terms of effectiveness, efficiency, stability and timeliness are obtained through randomised experiments with large-scale scenarios. The experimental results show that the method can be used for real-time conflict resolution in high-density 3D scenarios without causing significant domino effects.

4. 通过在大型场景中进行随机实验，获得了该方法在有效性、效率、稳定性和及时性方面的性能参数。实验结果表明，该方法可以在不引起显著多米诺效应的情况下，用于高密度三维场景中的实时冲突解决。

The rest of this paper is organised as follows. Section 2 describes and analyses the problem in detail. Section 3

proposes an operating framework for conflict management. Section 4 introduces the concept of airspace discretisation based on grids to improve the calculation efficiency. Section 5.1 proposes a method of autonomous planning of desired trajectory using visibility graph theory and the Dijkstra algorithm to avoid multiple restricted areas. Section 5.2 proposes a method of autonomous re-planning of optimal agreed trajectory. In Section 5.2, Section 5.2.3 establishes the fuel consumption model of the aircraft based on dynamics, referring to the Base of Aircraft Data (BADA) manual (EUROCONTROL, 2010); Section 5.2.4 establishes a time-space reachable model of the trajectory based on the space-time prism which can realise the visualisation of trajectories as well as evaluate the trajectory cost, and proposes a novel safety separation model based on multiple flight levels to resolve the trajectory conflict. A simulation is then conducted, and the numerical results are analysed in Section 6. Finally, Section 7 discusses the conclusions, the performance of the proposed method, and the directions for future research.

本文其余部分组织如下。第 2 节详细描述和分析问题。第 3 节提出了冲突管理的操作框架。第 4 节介绍了基于网格的空域离散化概念，以提高计算效率。第 5.1 节提出了一种使用可见性图理论和 Dijkstra 算法自主规划期望轨迹的方法，以避开多个受限区域。第 5.2 节提出了一种自主重新规划最优协商轨迹的方法。在第 5.2 节中，第 5.2.3 节根据动力学原理，参照《飞机数据基础》(BADA) 手册 (EUROCONTROL, 2010)，建立了飞机燃油消耗模型；第 5.2.4 节基于时空棱镜建立了轨迹的时间-空间可达模型，可以实现轨迹的可视化以及轨迹成本的评估，并提出了基于多个飞行高度层的新型安全间隔模型，以解决轨迹冲突。随后进行了模拟，并在第 6 节分析了数值结果。最后，第 7 节讨论了结论、提出方法的性能以及未来研究的方向。

2. Problem description and analysis

2. 问题描述与分析

The problem to be solved in this paper has the following characteristics:

本文要解决的问题具有以下特点:

1. With the help of CNS technologies, aircraft can operate autonomously according to preset trajectories, and aircraft in the airspace can share trajectories with each other.

1. 在 CNS 技术的帮助下，飞机可以根据预设轨迹自主运行，空域内的飞机可以相互共享轨迹。

2. Trajectory planning should meet the requirements of the TBO operation concept. Compared with traditional path planning, it is mainly reflected in the CTAs of waypoints and the need for trajectory recovery after rerouting.

2. 轨迹规划应满足 TBO 运行概念的要求。与传统路径规划相比，主要体现在航路点的 CTA 以及重新规划后的轨迹恢复需求上。

3. The airspace environment is FRA.

3. 空域环境是 FRA。

4. There are event-triggered temporary restricted areas in the airspace caused by hazardous weather, military activities, and other factors. In this paper, the event update is not included.

4. 空域中存在由恶劣天气、军事活动等因素引起的事件触发临时限制区域。本文不包括事件更新。

5. The trajectory planning calculation time should meet the real-time operation requirements.

5. 轨迹规划计算时间应满足实时运行要求。

6. Manoeuvres include changes of the heading, speed, flight level (FL), and any combination of them.

6. 操作包括改变航向、速度、飞行高度 (FL) 以及它们的任意组合。

7. Trajectory optimisation needs to meet multi-dimensional performance expectations, such as punctuality and economic expectations from the AU perspective and orderliness and safety expectations from the ATM perspective.

7. 轨迹优化需要满足多维性能期望，例如从 AU 角度看准时性和经济性期望，以及从 ATM 角度看有序性和安全性期望。

8. The solution of autonomous trajectory planning should be intuitively understandable.

8. 自主轨迹规划解决方案应直观易懂。

From an optimisation point of view, this is a large-scale constrained programming problem. It is a complex piecewise function extremum problem to judge the conflict of the rerouting trajectory considering the trajectory recovery and multi-flight levels, and it is difficult to construct a standard programming problem model. It is often necessary to enumerate all cases and construct the conflict relation matrix to represent the conflict relation between the trajectories, which is very time-consuming. In addition, the quantitative determination of the relationship between multiple optimisation objectives is also difficult. More importantly, considering interactions of human-machine/air-ground greatly limits the solution method of the problem, and a higher comprehensibility of the results of the rerouting planning is required. Therefore, it is very challenging to solve this problem well.

从优化角度看，这是一个大规模约束规划问题。在考虑轨迹恢复和多层飞行的情况下，判断重新规划轨迹的冲突是一个复杂的分段函数极值问题，难以构建标准的编程问题模型。通常需要枚举所有情况并

构建冲突关系矩阵来表示轨迹之间的冲突关系，这非常耗时。此外，多个优化目标之间关系的定量确定也困难。更重要的是，考虑到人机/空地交互大大限制了问题的解法，且重新规划结果的可理解性要求更高。因此，妥善解决这一问题极具挑战性。

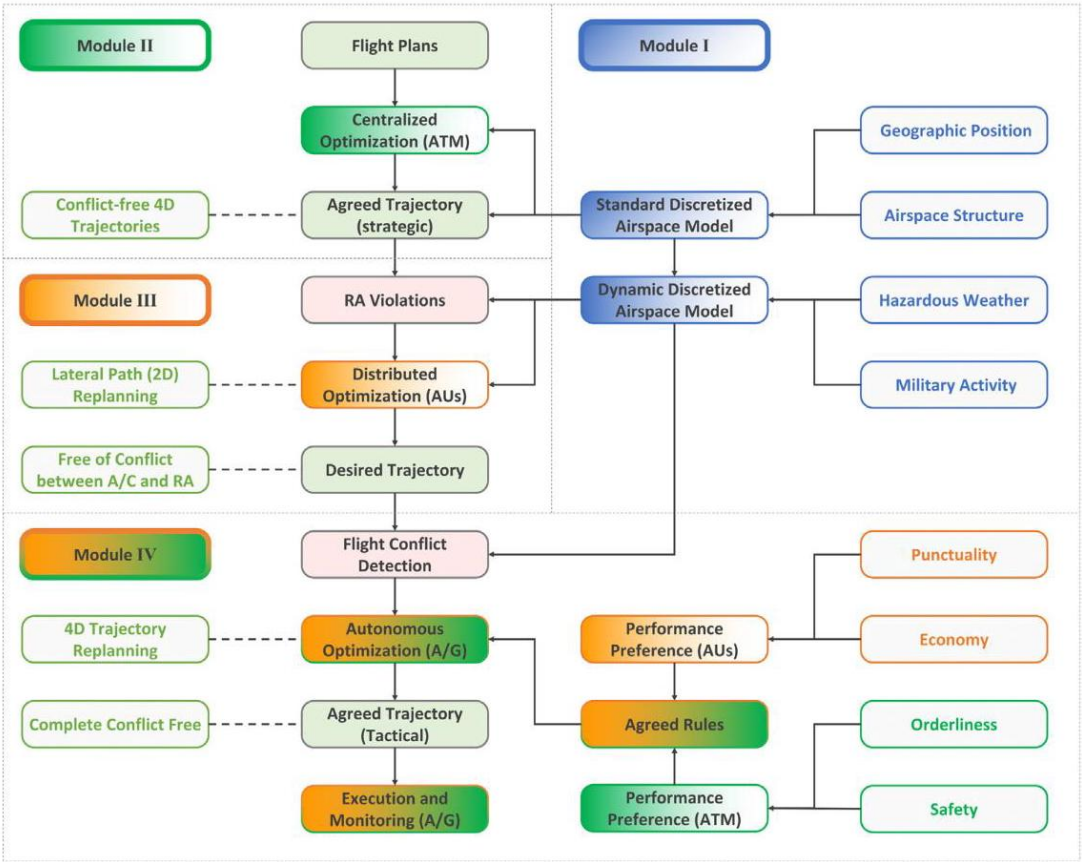

Fig. 1. Operational framework of autonomous trajectory operating system.
图 1. 自主轨迹操作系统的运行框架。

3. Operational framework of autonomous trajectory operating system

3. 自主轨迹操作系统的运行框架

In this work, the problem is divided into parts and that are solved individually. Therefore, a multi-module, multi-stage and complete technical approach was designed. Fig. 1 shows the operational framework of autonomous trajectory operating system. It is proposed to provide an integral picture to illustrate the operational procedures underpinned by a series of key required technologies. The operational framework is comprised of four modules, which are discussed in the following paragraphs.

在这项工作中，问题被划分为几个部分并分别解决。因此，设计了一种多模块、多阶段且完整的技术方法。图 1 展示了自主轨迹操作系统的运行框架。提出提供一个整体图像来阐述由一系列关键技术支撑的运行程序。运行框架包括四个模块，以下各段将对其进行讨论。

3.1. Module I : Grid-based airspace discretisation

3.1. 模块 I: 基于网格的空域离散化

In this module, the airspace is discretised based on static airspace information (such as geographic information data and airspace structure data) by the standard discretised airspace model. In real-time operation, the module generates a restricted area based on dynamic airspace information (such as hazardous weather and military activities) by the

dynamic discretised airspace model. It should be noted that all the restricted areas in this paper are temporary. Airspace discretisation based on grids not only helps to achieve situational awareness but also promotes the balance between the effect of the trajectory optimisation and calculation time.

在本模块中，空域基于静态空域信息 (如地理信息数据和空域结构数据) 通过标准离散空域模型进行离散化。在实时运行中，该模块通过动态离散空域模型，基于动态空域信息 (如有害天气和军事活动) 生成受限区域。需要注意的是，本文中的所有受限区域都是临时的。基于网格的空域离散化不仅有助于实现态势感知，也促进了轨迹优化效果与计算时间之间的平衡。

3.2. Module II : Initial conflict-free trajectory planning

3.2. 模块 II: 初始无冲突轨迹规划

This module is for the centralised control optimisation of the ATM according to the flight plans. In the strategic stage, considering airspace restrictions and flight conflicts, this module generates conflict-free agreed trajectories based on the flight plans of all AUs. It should be noted that the optimisation restrictions here do not include temporary restricted areas in real-time.

本模块用于根据飞行计划对空中交通管理 (ATM) 进行集中控制优化。在战略阶段，考虑到空域限制和飞行冲突，该模块基于所有航空单位 (AUs) 的飞行计划生成无冲突的协商轨迹。需要注意的是，这里的优化限制不包括实时中的临时受限区域。

3.3. Module III : Trajectory pre-planning based on temporary restricted area

3.3. 模块 III: 基于临时受限区域的轨迹预规划

This module is initiated by the AUs when they are about to enter the target airspace to generate a desired trajectory based on the temporary airspace restrictions and the previously agreed trajectory by only considering the restricted area (RA) constraints, regardless of the potential conflicts between aircraft. For the sake of simplicity, flight level-changes are not required in this module. A visibility graph and the Dijkstra algorithm are applied to update the lateral trajectory with the AU preferred airspeed.

当自主单元 (AUs) 即将进入目标空域时，此模块由它们启动，以根据临时空域限制和之前商定的轨迹仅考虑受限区域 (RA) 约束，生成期望轨迹，而不考虑飞机之间潜在的冲突。为了简化，此模块不要求飞行高度层变更。使用可见性图和迪杰斯特拉算法更新横向轨迹，以适应 AU 偏好的空速。

3.4. Module IV : Real-time conflict-free 4D trajectory re-planning

3.4. 模块 IV: 实时无冲突 4D 轨迹重规划

After entering the sector, this module is autonomously implemented by the aircraft following the conflict management agreement reached by the ATM and AUs to generate a real-time, conflict-free, agreed trajectory, which is monitored by ATM and AUs, that is, air-ground. This module includes a novel optimisation model and algorithm for CR. In the real world, ATM expects higher safety and orderliness, while AUs expect better economy and punctuality. To establish a more efficient and feasible optimisation model, this paper takes safety as a strong constraint, punctuality as a weak constraint, orderliness as a priority strategy, and only the economy as an optimisation objective to establish an optimisation model (Section 5.2). To make the solution intuitively understandable, the space-time prism theory in time geography and reachable solution space representation are applied to the CR method.

飞机进入扇区后，此模块会自主执行，遵循空中交通管理 (ATM) 和自主单元 (AUs) 达成的冲突管理协议，生成实时、无冲突、商定的轨迹，该轨迹由 ATM 和 AUs 监控，即空地监控。此模块包括用于冲突解决 (CR) 的新型优化模型和算法。在实际世界中，ATM 期望更高的安全和有序性，而 AUs 期望更好的经济性和准时性。为了建立一个更高效且可行的优化模型，本文将安全性作为强约束，准时性作为弱约束，有序性作为优先策略，并将经济性作为唯一的优化目标，建立了一个优化模型 (第 5.2 节)。为了使解决方案直观易懂，将时间地理学中的时空棱镜理论和可达解决方案空间表示法应用于 CR 方法。

We divide the trajectory planning during operation into two stages, that is pre-planning (Module III) and re-planing (Module IV). This is both for the compatibility with the current TBO mechanism and enabling more efficient

and optimal planning of trajectories. In the context of TBO, the 4D trajectory of the aircraft will be dynamically adjusted before and during the operation. The process of trajectory adjustment involves the submission of the desired trajectory and the determination of an agreed trajectory. Specifically, when the airspace situation changes, the ATM units will optimise the demand and capacity relationship by assigning regulated controlled time of arrivals (CTAs) to the affected flights. Then, a new desired 4D trajectory of each flight that avoids the restricted area will be submitted by airlines or pilots (where the internal negotiation may be required) before entering the restricted sector (i.e., function of Module III). The generation of the new CTAs involves demand and capacity balancing, which is a large-scale, time-consuming optimisation problem that is beyond the scope of this paper. Therefore, the Module III is designed to implement before entering the sector, (potentially) leaving sufficient time for DCB optimisation and coordination in practice. Otherwise, if we integrate pre-planning into the Module IV, the time to get a conflict-free trajectory will be delayed and thus the best time to reroute is likely to be missed.

我们将操作过程中的轨迹规划分为两个阶段，即预规划 (模块 III) 和重新规划 (模块 IV)。这样做既是为了与当前的 TBO 机制兼容，也是为了实现更高效和最优的轨迹规划。在 TBO 的背景下，飞机的 4D 轨迹将在操作前和操作期间动态调整。轨迹调整过程包括提交期望轨迹和确定协议轨迹。具体来说，当空域情况发生变化时，空管单位将通过为受影响的航班分配规定的控制到达时间 (CTA) 来优化需求与容量的关系。然后，在进入受限区域之前，航空公司或飞行员 (可能需要进行内部协商) 将提交每个航班避免受限区域的新 4D 期望轨迹 (即模块 III 的功能)。新 CTA 的生成涉及到需求与容量的平衡，这是一个大规模、耗时的优化问题，超出了本文的范围。因此，模块 III 被设计为在进入空域之前实施，(可能) 为实际中的 DCB 优化和协调留出足够的时间。否则，如果我们将预规划整合到模块 IV 中，获得无冲突轨迹的时间将会延迟，从而可能导致错过最佳改航时间。

This framework covers the whole process of flight trajectory planning. This paper mainly introduces the relevant models and algorithms of Modules I, III, and IV (Module II uses a common strategic 4D conflict-free trajectory planning method based on random flight schedules, which will not be elaborated on in this paper) (Ruiz et al., 2014).

该框架涵盖了整个飞行轨迹规划过程。本文主要介绍了模块 I、III 和 IV 的相关模型和算法 (模块 II 使用基于随机航班时刻表的通用战略 4D 无冲突轨迹规划方法，本文将不详细阐述)(Ruiz 等人，2014 年)。

4. Grid-based airspace discretisation (module I)

4. 基于网格的空域离散化 (模块 I)

In the context of TBO, airspace parameterisation is one of the necessary conditions. The airspace environment adopted in this paper is the FRA, which has a higher operational flexibility. Considering the actual operation situation, the aircraft can change its flight level when appropriate. Considering that the computational cost of the optimisation solution in continuous space is very expensive, in this framework, the airspace is discretised, which is also the core function of Module I.

在 TBO 的背景下，空域参数化是必要条件之一。本文采用的空域环境是 FRA，它具有更高的运行灵活性。考虑到实际运行情况，飞机在适当的时候可以改变其飞行高度。考虑到在连续空间中优化解决方案的计算成本非常高，在这个框架下，空域被离散化，这也是模块 I 的核心功能。

4.1. Airspace gridding in three dimensions

4.1. 三维空域划分

The need for aircraft to satisfy the CTA at key waypoints is the core requirement of TBO, that is, when the aircraft encounters a conflict, the aircraft needs to search for suitable rerouting waypoints, corresponding speeds, and flight levels to make the time for the aircraft to reach the entry and exit points of the sector meet the CTA requirements as much as possible. Since searching for accurate and optimal rerouting waypoints in continuous space is very time-consuming, based on latitude, longitude, and altitude, we divide the airspace into a series of neatly arranged 3D grids to discretise the airspace. In the vertical dimension, the height of the 3D grid is the vertical distance between adjacent FLs. In the horizontal dimension, the base of the 3D grid is square. By projecting the 3D grid of each layer down onto a two-dimensional (2D) plane, we obtain the corresponding 2D grid. Considering the time limit of real-time decision-making, a trade-off must be made between the optimisation accuracy and calculation speed. Airspace gridding is a convenient way to balance these two aspects, which we have discussed in our previous papers (Yutong et al., 2020).

飞机需要满足关键航路点上的 CTA 要求是 TBO 的核心要求，即当飞机遇到冲突时，飞机需要寻找合适的绕航航路点、相应的速度和飞行高度，以使飞机到达扇区进出口的时间尽可能满足 CTA 要求。由于

在连续空间中寻找准确和最优的绕航航路点非常耗时，基于纬度、经度和高度，我们将空域划分为一系列整齐排列的三维网格以离散化空域。在垂直维度上，三维网格的高度是相邻飞行高度层之间的垂直距离。在水平维度上，三维网格的底面是正方形。通过将每一层的三维网格投影到二维 (2D) 平面上，我们得到相应的二维网格。考虑到实时决策的时间限制，必须在优化精度和计算速度之间做出权衡。空域划分是平衡这两方面的便捷方式，我们已在之前的论文中讨论过这一点 (Yutong 等人，2020 年)。

4.2. Classification of grids

4.2. 网格分类

Grids are defined as three types: restricted, protected, and available (Fig. 2). The restricted grid is the grid occupied by the restricted area, which aircraft cannot fly into due to hazardous weather, military activities, and other influences. It must be particularly noted that, based on safety considerations, if there is restricted area within the grid, regardless of whether it is completely occupied, it will be identified as a restricted grid. The protected grid is the grid adjacent to a restricted grid. Protected grids may be single or multiple layers depending on the size of the 3D ground grid and the horizontal safety separation between the aircraft and the restricted area. If the grid size is greater than or equal to the required safety distance in some dimension, we only need to set up one layer of the protected grid; if not, we need to set up multiple protected grid layers for the safe separation, which ensures that the thickness of the protected grid layers cannot be less than the safe separation. The smaller the grid size is, the more accurate the representation of the airspace state will be. Another more direct way to set the protected grid is that if there is a position in a non-restricted grid and the distance between the position and a restricted area is less than the safe separation, the grid must be a protected grid. The available grid refers to the grids that can be used for aircraft flight in the airspace, that is, the grids in the airspace except for the restricted grid and the protected grid. Furthermore, the restricted grid and the protected grid are collectively referred to as the unavailable grid.

格网被定义为三种类型: 受限格网、保护格网和可用格网 (图 2)。受限格网是指被受限区域占据的格网，由于危险天气、军事活动等因素，飞机无法进入。特别需要注意的是，基于安全考虑，如果格网内存在受限区域，无论其是否完全占据，都将被识别为受限格网。保护格网是指紧邻受限格网的格网。保护格网可能是单层或多层，这取决于三维地面格网的大小以及飞机与受限区域之间的水平安全间隔。如果格网大小在某些维度上大于或等于所需的安全距离，我们只需要设置一层保护格网；如果不是，我们需要设置多层的保护格网以确保安全间隔，这保证了保护格网层的厚度不得小于安全间隔。格网越小，对空域状态的表示越精确。另一种设置保护格网的更直接的方法是，如果非受限格网中存在一个位置，且该位置与受限区域的距离小于安全间隔，则该格网必须是保护格网。可用格网是指可用于飞机在空域中飞行的格网，即除了受限格网和保护格网之外的空域格网。此外，受限格网和保护格网统称为不可用格网。

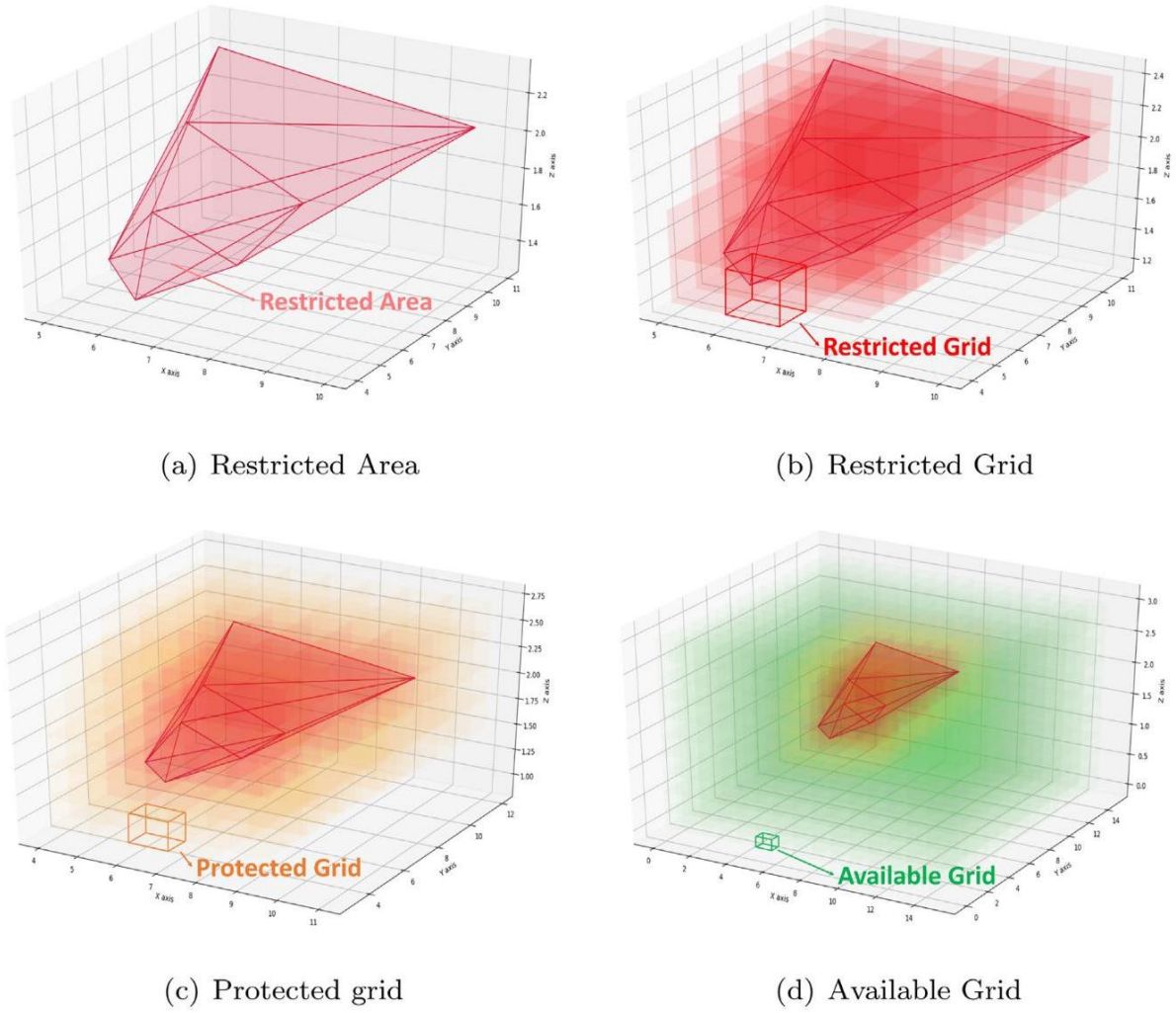

(a) Restricted Area (b) Restricted Grid

(c) Protected grid (d) Available Grid

Fig. 2. Diagrams of different types of grids.
图 2. 不同类型格网的示意图。

4.3. Coordinates of grids

4.3. 格网的坐标

For ease of use, we represent the key coordinates of the grid in two dimensions (Fig. 3). The eight vertices of a 3D grid can be viewed as four vertices of the upper and four vertices of the lower 2D grids. It is noted that the lower 2D grid type is the same as the 3D grid type. $C\left(X,Y,Z\right)$ is used to represent the 2D grid whose grid coordinates are $C\left(X,Y\right)$ and the flight level is Z . For any 2D grid, there are five key coordinate points, namely one centre point and four vertices. Supposing that the sides of the 2D grid are L , the vertical distance between adjacent flight levels is H , and the coordinates of the origin are (x_0, y_0, z_0) , then the actual coordinates of the five major locations of $C\left(X,Y,Z\right)$ can be expressed as follows, where $g_C, g_{NW}, g_{NE}, g_{SW}$, and g_{SE} represent the actual coordinates of the centre point and four vertices of the 2D grid, respectively:

为了使用方便，我们用二维 (图 3) 表示网格的关键坐标。三维网格的八个顶点可以看作是上层二维网格的四个顶点和下层二维网格的四个顶点。值得注意的是，下层二维网格类型与三维网格类型相同。$C\left(X,Y,Z\right)$ 用来表示网格坐标为 $C\left(X,Y\right)$ 且飞行高度为 Z 的二维网格。对于任何二维网格，有五个关键坐标点，即一个中心点和四个顶点。假设二维网格的边长为 L ，相邻飞行高度之间的垂直距离为 H ，原点的坐标为 (x_0, y_0, z_0) ，那么 $C\left(X,Y,Z\right)$ 的五个主要位置的实际坐标可以表示如下，其中 $g_C, g_{NW}, g_{NE}, g_{SW}$ 和 g_{SE} 分别代表 2D 网格的中心点和四个顶点的实际坐标:

$$g_C\left(X,Y,Z\right) = (x_0 + XL + L/2, y_0 + YL + L/2, z_0 + ZH) \tag{1}$$

$$g_{NW}\left(X,Y,Z\right)=\left(x_0+XL,y_0+YL+L,z_0+ZH\right) \tag{2}$$

$$g_{NE}\left(X,Y,Z\right)=\left(x_0+XL+L,y_0+YL+L,z_0+ZH\right) \tag{3}$$

$$g_{SW}\left(X,Y,Z\right)=\left(x_0+XL,y_0+YL,z_0+ZH\right) \tag{4}$$

$$g_{SE}\left(X,Y,Z\right)=\left(x_0+XL+L,y_0+YL,z_0+ZH\right) \tag{5}$$

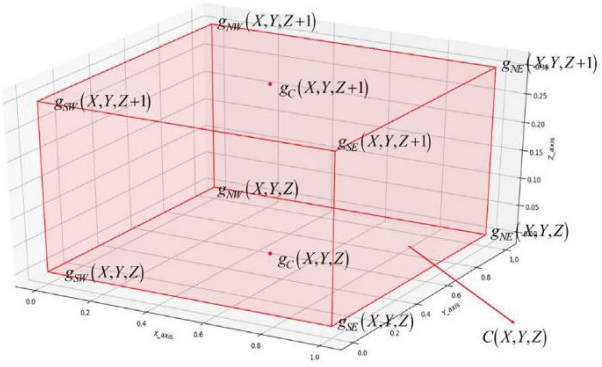

Fig. 3. Three-dimensional grid model.

图 3. 三维网格模型。

Among the five major locations, the centre point g_C will be used as a node in the visibility graph (refer to Section 5.1.1) and as a rerouting point in the autonomous re-planning for optimally agreed trajectory (refer to Section 5.2), while the four vertices g_{NW} , g_{NE}, g_{SW} , and g_{SE} will be used to discern whether a trajectory crosses the grid.

在这五个主要位置中，中心点 g_C 将被用作可见图 (参见 5.1.1 节) 中的节点，以及在自主重新规划中作为优化同意轨迹的重新路由点 (参见 5.2 节)，而四个顶点 g_{NW} 、g_{NE}, g_{SW} 和 g_{SE} 将被用来判断轨迹是否穿过网格。

Airspace discretisation based on grids is the operating basis of the operating framework proposed in this paper. Compared with the ordinary airspace environment, its advantages are as follows:

基于网格的空域离散化是本文提出的操作框架的操作基础。与普通空域环境相比，其优点如下:

1. There are usually three types of aircraft manoeuvring methods commonly used by controllers. They are: changing the heading, flight level, and flight speed. One more could be a combination thereof (Wang et al., 2020). In the operating environment proposed in this paper, when the grid-based rerouting waypoint is selected, combined with the aircraft's entry and exit points in the airspace and their CTA, which are determined according to the flight plan, the aircraft's heading, flight level, and flight speed can be calculated. This can effectively support the optimisation of continuous space problems with reasonable accuracy (Yutong et al., 2020).

1. 控制员通常使用三种飞机机动方法，它们是: 改变航向、飞行高度和飞行速度。另外一种可能是上述方法的组合 (Wang et al., 2020)。在本文提出的运行环境中，当选择基于网格的重新路由航点时，结合飞机在空域的入口和出口点以及它们的 CTA(根据飞行计划确定)，可以计算出飞机的航向、飞行高度和飞行速度。这可以有效地支持连续空间问题的优化，并具有合理的精度 (Yutong et al., 2020)。

2. Through airspace discretisation, the calculation time and optimisation accuracy can be flexibly balanced, so that they can satisfy both the real-time operation requirements and safe separation.

2. 通过空域离散化，可以灵活地平衡计算时间和优化精度，以满足实时运行需求和安全的间隔要求。

3. Because of the ordered arrangement of the grid, the usually irregular restricted area (especially those caused by hazardous weather) are converted into relatively regular geometric figures, so that the visibility graph can be better used (refer to Section 5.1.1).

3. 由于网格的有序排列，通常不规则的受限区域 (尤其是由恶劣天气引起的) 被转换为相对规则的几何图形，因此可以更好地使用可见性图 (参见第 5.1.1 节)。

4. The number of layers of protected grids can be flexibly adjusted to suit the different safety preferences of ATM

4. 受保护网格的层数可以根据空中交通管理 (ATM) 的不同安全偏好灵活调整。

It should be noted that the dynamic discretised airspace model in the framework is dynamically updated. This update is event-triggered. Event-triggered means that the dynamic discretised airspace model will be updated when military activities and hazardous weather result in the changes to restricted areas or when ATM modifies safety

performance preferences resulting in changes to protected areas. It should be noted that the protected grid serves as a buffer that can cope with the movement of hazardous weather areas for a limited period (Alonso-Ayuso et al., 2010). Considering that the framework of the autonomous trajectory operation system has been described (refer to Section 3), in the following, we will discuss the methodology of our CD&R method within a single airspace model update cycle.

应该注意的是，框架中的动态离散空域模型是动态更新的。这种更新是事件触发的。事件触发意味着当军事活动或恶劣天气导致受限区域发生变化，或者 ATM 修改安全性能偏好导致保护区域变化时，动态离散空域模型将会更新。应该注意的是，保护网格作为缓冲区，可以在有限时间内应对恶劣天气区域的变化 (Alonso-Ayuso et al., 2010)。考虑到自主轨迹操作系统框架已经描述过 (参见第 3 节)，在接下来的内容中，我们将讨论在单个空域模型更新周期内我们的 CD&R 方法。

5. Autonomous optimal planning of four-dimensional (4D) trajectory in restricted airspace

5. 四维 (4D) 航迹在受限空域中的自主最优规划

The goal of TBO is to generate a conflict-free 4D trajectory that meets the airport and airspace capacity constraints through continuous trajectory negotiation before takeoff. However, in actual operation, affected by temporary and dynamic hazardous weather and military activities, real-time negotiation and adjustment of the flight trajectory during a flight is inevitable. It should be noted that it is time-consuming and inefficient to centrally plan a conflict-free 4D trajectory that satisfies the respective preferences for all aircraft that are about to enter the airspace, i.e., global optimisation. Therefore, we propose a two-stage real-time autonomous 4D trajectory planning method, as follows: stage one: the autonomous desired trajectory planning method based on the network (this is the core function of Module III, Section 5.1) and stage two: the autonomous agreed trajectory re-planning based on the space-time prism (this is the core function of Module IV, Section 5.2).

TBO 的目标是在起飞前通过连续的航迹谈判生成一个无冲突的 4D 航迹，满足机场和空域容量限制。然而，在实际运行中，受临时性和动态性的恶劣天气和军事活动影响，飞行过程中对航迹的实时谈判和调整是不可避免的。需要注意的是，为中心规划一个满足所有即将进入空域的飞机各自偏好的无冲突 4D 航迹，即全局优化，是耗时且低效的。因此，我们提出了一种两阶段的实时自主 4D 航迹规划方法，如下: 第一阶段: 基于网络的自主期望航迹规划方法 (这是模块 III 第 5.1 节的核心功能)，第二阶段: 基于时空棱柱的自主协商航迹重规划方法 (这是模块 IV 第 5.2 节的核心功能)。

5.1. Stage one: Autonomous planning of desired trajectory (module III)

5.1. 第一阶段: 自主规划期望航迹 (模块 III)

Before the aircraft enters the target airspace, it is important to update the existing agreed trajectory to the desired trajectory that meets the constraints of the restricted area (we call this process the ”adjustment process”). It is expected that trajectory planning needs to rely on air-ground to share airspace data, especially the location and geometric configuration of the restricted area. AUs can effectively plan the shortest flight path and corresponding flight speed under the constraints of the restricted area according to the airspace information, aircraft performance, and personal preferences of the pilot. Because this trajectory planning does not consider the change of the flight level, to facilitate analysis, this paper assumes that the pilots have a consistent preference, which is flying along the shortest path at the AU preferred airspeed. It should be noted that the desired trajectory only considers the constraints of the restricted area and does not consider the constraints between aircraft, so the desired trajectory is not necessarily a conflict-free trajectory.

在飞机进入目标空域之前，更新现有约定的轨迹至符合限制区域约束的期望轨迹是非常重要的 (我们称此过程为“调整过程”)。预计轨迹规划需要依赖空地共享空域数据，尤其是限制区域的位置和几何配置。在空域信息、飞机性能和飞行员个人偏好的约束下，自主系统 (AUs) 能够有效地规划出限制区域内的最短飞行路径和相应的飞行速度。由于这种轨迹规划没有考虑飞行高度的变化，为了便于分析，本文假设飞行员有一个一致的偏好，即沿着自主系统偏好的飞行速度的最短路径飞行。需要注意的是，期望轨迹仅考虑了限制区域的约束，并没有考虑飞机之间的约束，因此期望轨迹不一定是无冲突的轨迹。

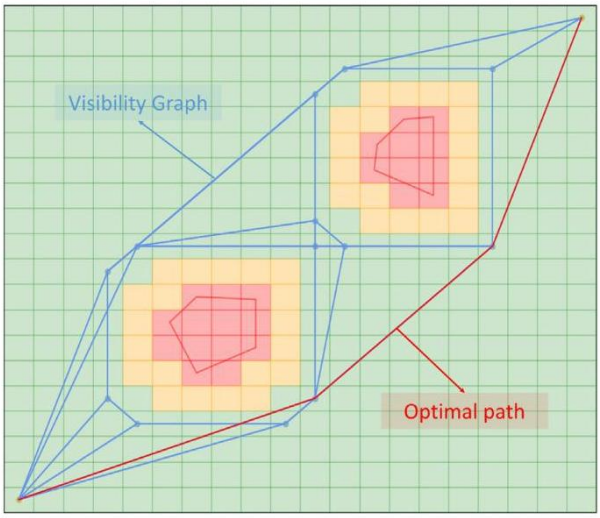

Fig. 4. Schema of visibility graph.
图 4. 可见性图示。

5.1.1. Visibility graph

5.1.1. 可见性图

Based on the above requirements, the visibility graph is introduced into path planning to search for the shortest flight path constrained by the restricted area effectively and intuitively (Lozano-Pérez and Wesley, 1979). The construction method of the visibility graph is as follows (Fig. 4): the starting point, the endpoint of the path to be searched, and the vertices of the convex boundary of the restricted area are used as points, and the line segments that do not pass through the restricted area connected by these points are used as edges to form an undirected graph, which is the visibility graph (Kaluder et al., 2011).

基于以上要求，将可见性图引入路径规划中，以有效直观地搜索受限制区域约束的最短飞行路径(Lozano-Pérez 和 Wesley，1979)。可见性图的构建方法如下 (图 4): 将搜索路径的起点、终点以及限制区域凸边界的顶点作为点，将这些点之间不穿过限制区域的线段作为边，形成一个无向图，这就是可见性图(Kaluder 等，2011)。

$G(V, E, \varphi)$ is used to represent the composition of a visibility graph, where V and E represent the sets of all vertices and edges in the graph, respectively, and φ represents the corresponding rule of the vertices and edges. Based on airspace gridding, each aircraft can generate a visibility graph on the 2D grid at its flight level. V_1 is used for the set of vertices in the area of the unavailable grid:

$G(V, E, \varphi)$ 用于表示可见性图的组成，其中 V 和 E 分别代表图中所有顶点和边的集合，φ 代表顶点和边的相应规则。基于空域格网化，每架飞机都能够在其飞行高度上的 2D 格网上生成一个可见性图。V_1 用于表示不可用格网区域内的顶点集合:

$$V_1 = \left\{ \begin{array}{l} P_v = g_C(X, Y, Z), \\ \exists! C(X', Y', Z) \in U_Z : |X - X'| = |Y - Y'| = 1, \\ \forall C(X'', Y'', Z) \notin U_Z : |X - X''| + |Y - Y''| = 1 \end{array} \right\} \tag{6}$$

where v is a vertex of the graph, P_v represents the actual coordinates of v , and U_Z is the 2D unavailable grid at flight level z . V_1 is then used for the set of entry and exit points, where P_I and P_O are the entry and exit points of the aircraft in the airspace, respectively. Therefore, V_1 and V_2 together constitute the vertices of the graph:

其中 v 是图中的一个顶点，P_v 代表 v 的实际坐标，U_Z 是飞行高度上的二维不可用格网。V_1 用于表示入口和出口点的集合，其中 P_I 和 P_O 分别代表飞机在空域中的入口和出口点。因此，V_1 和 V_2 共同构成了图的顶点:

$$V_2 = \{v \mid P_v = P_I \text{ or } P_O\} \tag{7}$$

$$V = V_1 \cup V_2 \tag{8}$$

The set of edges and corresponding rule can be represented as follows, where e is an edge of the graph, and $|v_i v_j|$ represents the line between v_i and v_j . The edges of the visibility graph are undirected, and their weights depend on their actual distance. The above is the construction method of the visibility graph, and through this method, we obtain an undirected weighted graph.

边的集合及其相应规则可以表示如下，其中 e 是图中的一条边，$|v_i v_j|$ 代表 v_i 和 v_j 之间的直线。可见性图的边是无向的，它们的权重取决于它们的实际距离。以上是可见性图的构建方法，通过这种方法，我们获得了一个无向加权图。

$$E = \{e \mid \varphi(e) = \langle v_i, v_j \rangle, v_i, v_j \in V\} \tag{9}$$

$$\varphi(e) = \langle v_i, v_j \rangle : \forall C(X,Y,Z) \cap |v_i v_j| = \varnothing, C(X,Y,Z) \in U_Z \tag{10}$$

5.1.2. Dijkstra algorithm for desired trajectory search

5.1.2. 迪杰斯特拉算法在期望轨迹搜索中的应用

The Dijkstra algorithm is the shortest path algorithm from one vertex to the other vertices, and it solves the shortest path problem on a suitable graph (Dijkstra et al., 1959). It starts from a starting point and uses a greedy algorithm. For each step, it moves to the adjacent node of the vertex that is closest to the starting point and has not been visited until it expands to the endpoints. For small-scale graphs, the Dijkstra algorithm can quickly calculate the globally shortest path. Therefore, based on the visibility graph, the Dijkstra algorithm is used to search for the shortest path in the undirected weighted graph generated above.

Dijkstra 算法是从一个顶点到其他顶点的最短路径算法，它解决了在适合的图上的最短路径问题 (Dijkstra 等人，1959 年)。它从起点开始，使用贪心算法。每一步，它移动到距离起点最近且未被访问的顶点的相邻节点，直到扩展到端点。对于小规模图，Dijkstra 算法可以快速计算出全局最短路径。因此，基于可视图，使用 Dijkstra 算法在上述生成的无向加权图中搜索最短路径。

The autonomous planning of the desired trajectory method is shown in Algorithm 1, which can generate the optimal desired trajectory based on the standard and dynamic discretised airspace model. Among them, N_X and N_Y represent the number of X - direction and Y -direction grids respectively, len (V_{vertex}) represents the number of elements in V_{vertex} , and $V_{\text{vertex}}[i]$ and $V_{\text{vertex}}[j]$ represent the i th and j th element in V_{vertex} respectively. For an aircraft, the set of vertices and the set of visibility graph are initialled first (line 1). Then, the vertices of the unavailable area are constructed (lines 2-9). Next, the set of visibility graph edges is constructed (lines 9-17) based on the visibility of any two points in the set of vertices. Finally, the shortest trajectory is found (line 18) as the desired trajectory of the aircraft by the Dijkstra algorithm.

所需轨迹的自主规划方法如算法 1 所示，它可以根据标准和动态离散的空域模型生成最优的所需轨迹。其中，N_X 和 N_Y 分别代表 X 方向和 Y 方向的网格数，len (V_{vertex}) 代表 V_{vertex} 中的元素数量，$V_{\text{vertex}}[i]$ 和 $V_{\text{vertex}}[j]$ 分别代表 V_{vertex} 中的第 i 个和第 j 个元素。对于一架飞机，首先初始化顶点集合和可视图集合 (第 1 行)。然后，构建不可用区域的顶点 (第 2-9 行)。接下来，基于顶点集合中任意两点之间的可视性，构建可视图边集合 (第 9-17 行)。最后，通过 Dijkstra 算法找到最短轨迹 (第 18 行)，作为飞机的所需轨迹。

Algorithm 1 Autonomous planning of desired trajectory

算法 1 自主规划所需轨迹

Input: entry point coordinates V_I and exit point coordinates V_O of the aircraft, as well as the airspace date.

1: initialise the set of vertices V_{vertex} and the set of visibility graph V_{visible}
append v_I and v_O to v_{vertex}
for X from 0 to N_X do
  for Y from 0 to N_Y do
    if $C(X,Y)$ is a vertex of the area of the unavailable grid then
      append $C(X,Y)$ to V_{vertex}
    end if
  end for
end for
  for i from 0 to len $(V_{\text{vertex}}) - 1$ do
  for j from i to len (V_{vertex}) do
    connect $V_{\text{vertex}}[i]$ and $V_{\text{vertex}}[j]$ to form the segment $|v_i v_j|$

if $|v_i v_j|$ is visible then
append $|v_i v_j|$ to V_{visible}
end if
end for
end for
18: Take v_I and v_O as starting and ending point respectively, search the shortest path in V_{visible} by Dijkstra Algorithm as
trajectory $_{\text{desired}}$ of the aircraft
Output: trajectory desired

5.2. Stage two: Autonomous re-planning of optimal agreed trajectory (module IV)

5.2. 第二阶段: 最优协商轨迹的自主重新规划 (模块 IV)

After the aircraft enters the target airspace, since the desired trajectory may not be a conflict-free trajectory, the aircraft will detect potential trajectory conflicts based on the airspace traffic situation shared by the air-ground and the flight intention information. If there is no conflict, the aircraft will first fly along the desired trajectory; otherwise, it will quickly and autonomously re-plan a conflict-free 4D agreed trajectory.

在飞机进入目标空域后，由于期望轨迹可能不是无冲突的轨迹，飞机将根据空地共享的空域交通情况和飞行意图信息检测潜在的轨迹冲突。如果没有冲突，飞机将首先沿着期望轨迹飞行；否则，它将快速自主地重新规划一条无冲突的 4D 协议轨迹。

5.2.1. Optimisation strategy

5.2.1. 优化策略

In the operational framework proposed in this paper, the aircraft operates autonomously at this stage based on an agreement reached between ATM and AUs. This paper proposes a single-objective optimisation model based on the flight cost. The aircraft direct operating cost usually encompasses a weighted sum of fuel consumption, route charges, and time-related costs (such as crew and maintenance fees) (Xu et al., 2020). Here, time is used as a constraint, in other words, the time for the aircraft to reach the point of entry and exit its target airspace is fixed. Therefore, time-related costs are constant. Because the optimisation scope of this model is a sector, the route charges are also constant within the same sector. Therefore, fuel consumption is taken as the optimisation target of this model.

在本文提出的运行框架中，飞机在此阶段根据 ATM 和 AUs 之间达成的协议自主运行。本文提出了基于飞行成本的单一目标优化模型。飞机的直接运行成本通常包括燃料消耗、航线费用和时间相关成本 (如机组人员和维护费用) 的加权总和 (Xu et al., 2020)。在这里，时间被用作约束条件，换句话说，飞机到达入口点和离开目标空域的时间是固定的。因此，时间相关成本是常数。由于该模型的优化范围是一个扇区，所以同一扇区内的航线费用也是常数。因此，燃料消耗成为该模型的优化目标。

It should be noted that the orderliness of the airspace is positively correlated with the efficiency of airspace operations (Kupfer et al., 2008). Furthermore, the separation of the priority function and the resolution function of flights can further promote the improvement of the airspace operation efficiency (Hoekstra et al., 2002). Therefore, this paper adopts the first-come-first-served strategy (Wu and Liu, 1994), that is, the aircraft that enters the airspace first has the priority to choose the trajectory. Based on this, when the aircraft enters the airspace, it only needs to plan a conflict-free trajectory based on the trajectory intent shared by the previous flights, and there is no need to adjust the trajectory again during the flight. This will ensure that each aircraft undergoes at most one rerouting, which will help the orderliness of the airspace.

应当注意的是，空域的有序性与空域运行效率呈正相关 (Kupfer 等人，2008 年)。此外，将航班的优先级函数与解决函数分离，可以进一步促进空域运行效率的提高 (Hoekstra 等人，2002 年)。因此，本文采用先来先服务策略 (Wu 和 Liu，1994 年)，即首先进入空域的飞机具有选择航迹的优先权。基于此，当飞机进入空域时，只需根据前序航班共享的航迹意图规划无冲突航迹，飞行过程中无需再次调整航迹。这将确保每架飞机最多经历一次重新路由，这将有助于空域的有序性。

Table 2

表 2
Explanation of symbols.
符号说明。

Symbols	Description
p	Atmospheric pressure
p_0	Standard atmospheric pressure at mean sea level
T	Temperature
T_0	Standard atmospheric temperature at mean sea level
g_0	Gravitational acceleration
β	International standard atmosphere temperature gradient with altitude below the tropopause
R	Real gas constant for air
H	Geopotential altitude
ρ	Air density
R_{OCD}	Rate of climb or descent
$\frac{d}{dt}$	Time derivative
Thr	Thrust acting parallel to the aircraft velocity vector
D	Drag force
V_{TAS}	True airspeed
S	Reference wing surface area
m	Aircraft mass
C_D	Drag coefficient
$C_{D0,CR}$	Parasitic drag coefficient (cruise)
$C_{D2,CR}$	Induced drag coefficient (cruise)
C_L	Lift coefficient
f_{cr}	Cruise fuel flow
η	Thrust specific fuel flow
C_{fcr}	Cruise fuel flow correction coefficient
C_{f1}	1st thrust specific fuel consumption coefficient
$\mathbf{C}_{f2}$	2nd thrust specific fuel consumption coefficient

符号	描述
p	大气压
p_0	平均海平面标准大气压
T	温度
T_0	平均海平面标准大气温度
g_0	重力加速度
β	国际标准大气温度梯度，随海拔变化至对流层顶以下
R	空气的实际气体常数
H	地势高度
ρ	空气密度
R_{OCD}	上升或下降率
$\frac{d}{dt}$	时间导数
推力	与飞机速度矢量平行的推力作用
D	阻力
V_{TAS}	真空速
S	参考翼表面积
m	飞机质量
C_D	阻力系数
$C_{D0,CR}$	漫游寄生阻力系数
$C_{D2,CR}$	漫游诱导阻力系数
C_L	升力系数
f_{cr}	漫游燃油流量
η	推力特定燃油流量
C_{fcr}	漫游燃油流量修正系数
C_{f1}	第一推力特定燃油消耗系数
$\mathbf{C}_{f2}$	第二推力特定燃油消耗系数

5.2.2. Decision variable

5.2.2. 决策变量

In this optimisation model, the decision variable is the grid coordinates of Rerouting Point (RP) which is represented as(X, Y, Z). Among them, X, Y and Z are integers and

在此优化模型中，决策变量是重新规划点 (RP) 的网格坐标，表示为 (X, Y, Z)。其中，X, Y 和 Z 是整数，

$$X \in [X_{\min}, X_{\max}] \tag{11}$$

$$Y \in [Y_{\min}, Y_{\max}] \tag{12}$$

$$Z \in \{Z_{\text{initial}} - 2, Z_{\text{initial}}, Z_{\text{initial}} + 2\} \tag{13}$$

where $X_{\min}$ and $X_{\max}$ are the minimum and maximum grid X coordinate respectively, $Y_{\min}$ and $Y_{\max}$ are the minimum and maximum grid Y coordinate respectively, and Z_{initial} is the initial flight level of the aircraft.

其中 $X_{\min}$ 和 $X_{\max}$ 分别是网格 X 坐标的最小值和最大值，$Y_{\min}$ 和 $Y_{\max}$ 分别是网格 Y 坐标的最小值和最大值，Z_{initial} 是飞机的初始飞行高度。

5.2.3. Objective function

5.2.3. 目标函数

The calculation of the fuel consumption uses the model provided in the BADA manual (EUROCONTROL, 2010). Because accurate fuel consumption calculations are not within the scope of this paper, to simplify the model, this paper makes the following assumptions:

燃料消耗的计算使用 BADA 手册中提供的模型 (EUROCONTROL，2010 年)。由于精确的燃料消耗计算不在本文的范围内，为了简化模型，本文做出以下假设:

(a) The horizontal true airspeed is constant.

(a) 水平真实空速是恒定的。

(b) The aircraft maintains a constant climb/descent rate during the climb/descent process, that is, the vertical true airspeed is constant.

(b) 飞机在爬升/下降过程中保持恒定的爬升/下降率，即垂直真实空速是恒定的。

(c) The change of the aircraft speed is instantaneous.

(c) 飞机速度的变化是瞬时的。

(d) The air environment is the international standard atmosphere.

(d) 空气环境是国际标准大气。

(e) The wind factor is not considered.

(e) 未考虑风的影响因素。

(f) The flight levels considered were between FL310 and FL360.

(f) 考虑的飞行高度在 FL310 至 FL360 之间。

(g) The bank angle was not considered.

(g) 未考虑横滚角。

The symbols from BADA that are used below are shown in Table 2.

以下使用的来自 BADA 的符号在表 2 中显示。

Based on the above assumptions and BADA manual, the actual pressure model is given by (14):

基于上述假设和 BADA 手册，实际压力模型由 (14) 给出:

$$p = p_0 \left(\frac{T}{T_0} \right)^{-\frac{g_0}{\beta R}} \tag{14}$$

The temperature model is given by (15):

温度模型由 (15) 给出:

$$T = T_0 + \beta H \tag{15}$$

It is noted that, due to assumption (d), the geopotential altitude is equal to the geopotential pressure altitude. The air density model

注意到，由于假设 (d)，重力势高度等于重力势压力高度。空气密度模型
is given by (16):
由 (16) 给出:

$$\rho = \frac{p}{RT} \tag{16}$$

The vertical movement model is given by (17):
垂直运动模型由 (17) 给出:

$$R_{OCD} = \frac{dH}{dt} = \frac{(Thr - D) \cdot V_{TAS}}{mg_0} \tag{17}$$

The aerodynamic drag model is given by (18):
气动阻力模型由 (18) 给出:

$$D = \frac{C_D \cdot \rho \cdot {V_{TAS}}^2 \cdot S}{2} \tag{18}$$

Among (18), the drag and lift coefficients C_D and C_L are given by (19) and (20), respectively:
在 (18) 中，阻力系数和升力系数 C_D 和 C_L 分别由 (19) 和 (20) 给出:

$$C_D = C_{D0,CR} + C_{D2,CR} \times (C_L)^2 \tag{19}$$

$$C_L = \frac{2 \cdot m \cdot g_0}{\rho \cdot {V_{TAS}}^2 \cdot S} \tag{20}$$

The cruising fuel consumption rate model (per unit time) is given by (21):
巡航燃油消耗率模型 (单位时间) 由 (21) 给出:

$$f_{cr} = \eta \times Thr \times C_{fcr} \tag{21}$$

Where η is given by (22):
其中 η 由 (22) 给出:

$$\eta = C_{f1} \times \left(1 + \frac{V_{TAS}}{C_{f2}}\right) \tag{22}$$

However, and due to the assumption (a), (23) applies
然而，由于假设 (a)，(23) 适用

$$Thr = D \tag{23}$$

The cruising fuel consumption rate model is given by (24):
巡航燃油消耗率模型由 (24) 给出:

$$f_{cr} = \eta \times D \times C_{fcr} \tag{24}$$

Therefore, the cruising fuel consumption model is given by (25) where l_{cr} is the cruising distance of the aircraft:
因此，巡航燃油消耗模型由 (25) 给出，其中 l_{cr} 是飞机的巡航距离:

$$F_{cr} = \frac{l_{cr}}{V_{TAS}} f_{cr} \tag{25}$$

Due to assumption (b) and the above models, the climbing/descending fuel consumption model (from t_1 to t_2) is given by (26):
由于假设 (b) 和上述模型，爬升/下降燃油消耗模型 (从 t_1 到 t_2) 由公式 (26) 给出:

$$F_{cli/des} = \eta \int_{t_1}^{t_2} \left[\begin{array}{l} A \times (T_0 + \beta H_0 + \beta R_{OCD} t)^{E+1} + \\ B \times (T_0 + \beta H_0 + \beta R_{OCD} t)^{-E-1} + C \end{array} \right] dt \tag{26}$$

where the terms E, A, B and C are given by (27),(28),(29) and (30), respectively:
其中项 E, A, B 和 C 分别由公式 (27)、(28)、(29) 和 (30) 给出:

$$E = \frac{g_0}{\beta R} \tag{27}$$

$$A = \frac{2C_{D2,CR}m^2{g_0}^2R}{{V_{TAS}}^2Sp_0{T_0}^E} \tag{28}$$

$$B = \frac{C_{D0,CR}{V_{TAS}}^2Sp_0{T_0}^E}{2R} \tag{29}$$

$$C = \frac{R_{OCD}mg_0}{V_{TAS}} \tag{30}$$

Regrouping (26) and by substituting the values of the terms E, A, B and C leads to (31) where t_1 and t_2 are the start and end time

通过重新组合 (26) 并替换项 E, A, B 和 C 的值，得到 (31)，其中 t_1 和 t_2 分别是爬升/下降的起始和结束时间

of climb/descend, respectively,

分别对应。

$$F_{\text{cli / des}} = \eta\left[\frac{\frac{A}{\beta R_{\text{OCD}}(E+2)} \times (T_0 + \beta H_0 + \beta R_{\text{OCD}}\, t)^{E+2} -}{\frac{B}{\beta R_{\text{OCD}}\, E} \times (T_0 + \beta H_0 + \beta R_{\text{OCD}}\, t)^{-E} + C \times t}\right]_{t_1}^{t_2} \tag{31}$$

This model can be represented by (32):

此模型可以表示为 (32):

$$F_{\text{cli / des}} = \begin{cases} F_{\text{cli}} & R_{\text{OCD}} > 0 \\ F_{\text{des}} & R_{\text{OCD}} < 0 \end{cases} \tag{32}$$

The derivation of the fuel climbing/descending consumption model will not be presented in detail. Interested readers can refer to the BADA manual (EUROCONTROL, 2010) and the above assumptions, where the model is simply derived through integral theory. Additionally, it is noted that, in actual operation, the aircraft usually has a constant Mach number in the climbing/descending process; in this paper, a constant true airspeed is adopted. However, through simulation calculations, it is found that there is little difference in the fuel consumption (Considering that in this method, the height variation of aircraft is at most 2000 ft (Section 5.2.4), and the flight distance in a single sector is hundreds of kilometers (Section 6.1), this difference only accounts for about 0.1% of the fuel consumption), and the trend is the same under the two operating modes. To summarise, the objective function based on fuel consumption can be expressed by (33), where Z_{obj} is the objective function and $F_{\text{total}}\ (X, Y, Z)$ is the total fuel consumption of the aircraft based on its rerouting point(X, Y, Z):

燃料爬升/下降消耗模型的推导将不会详细呈现。感兴趣的读者可以参考 BADA 手册 (EUROCONTROL, 2010) 及上述假设，其中模型是通过积分理论简单推导得出的。此外，需要注意的是，在实际操作中，飞机在爬升/下降过程中通常保持恒定的马赫数；本文采用恒定真实空速。然而，通过模拟计算发现，燃料消耗差异很小 (考虑到在此方法中，飞机的高度变化最多为 2000 英尺 (第 5.2.4 节)，单个扇区的飞行距离达数百公里 (第 6.1 节)，这种差异仅占燃料消耗的大约 0.1%)，两种运行模式下的趋势相同。总之，基于燃料消耗的目标函数可以表示为 (33)，其中 Z_{obj} 是目标函数，$F_{\text{total}}\ (X, Y, Z)$ 是基于飞机的重新路由点 (X, Y, Z) 的总燃料消耗:

$$\begin{aligned} \min Z_{obj} &= F_{\text{total}}\ (X, Y, Z) \\ &= \begin{cases} F_{cr} & Z = Z_{\text{initial}} \\ F_{cr} + F_{cli} + F_{des} & \text{others} \end{cases} \end{aligned} \tag{33}$$

It should be noted that, in Section 5.2.3, (14)-(22) can be found directly or indirectly in BADA manual (EUROCONTROL, 2010) and other formulas were derived independently by ourselves.

应该注意的是，在第 5.2.3 节中，(14)-(22) 可以直接或间接在 BADA 手册 (EUROCONTROL，2010) 中找到，其他公式是由我们自己独立推导的。

5.2.4. Constraints

5.2.4. 约束条件

Before listing and discussing the problem constraints, the supplementary assumptions for the operation method are first established as follows:

在列出和讨论问题约束之前，首先建立操作方法的补充假设如下:

(h) Aircraft flying eastward are at odd-numbered flight levels, and aircraft flying westward are at even-numbered flight levels.

(h) 向东飞行的飞机位于奇数飞行高度层，向西飞行的飞机位于偶数飞行高度层。

(i) When an aircraft needs to change its flight level to avoid conflicts, it can only change to the two flight levels closest to its current flight level where the flight direction is the same as the current flight level, if conditions permit.

(i) 当飞机需要改变飞行高度以避免冲突时，在条件允许的情况下，它只能改变到与其当前飞行高度最接近的两个飞行高度，且飞行方向与当前飞行高度相同。

(j) The aircraft that changes the flight level must return to the default flight level before arriving at the exit point of the target airspace.

(j) 改变飞行高度的飞机必须在到达目标空域出口点之前返回默认飞行高度。

(k) The performance of the CNS can meet the precision requirements.

(k) CNS 的性能可以满足精度要求。

The constraints of the model consist of time, space, and flight performance. The time constraints include CTA constraints; the space constraints include flight conflict as well as restricted area constraints; and the flight performance constraints include turning angle as well as maximum/minimum flight speed constraints.

模型的约束包括时间、空间和飞行性能。时间约束包括 CTA 约束；空间约束包括飞行冲突以及限制区域约束；飞行性能约束包括转弯角度以及最大/最小飞行速度约束。

CTA constraint. The time for the aircraft to reach the entry and exit points of the target airspace needs to satisfy the CTA constraint. To make the solution understandable and to ensure that each aircraft undergoes at most one rerouting, we use space-time prism theory in the time geography (Miller, 1991; Klomp et al., 2015, 2019). Through the space-time prism model based on CTA, it can be deduced that the potential rerouting path of the aircraft exists in a specific elliptical space-time reachable area. Considering assumption (a), this constraint can be constructed from a 2D perspective. The grid coordinates(X, Y)are the decision variables, the coordinates(x, y)are the coordinates of rerouting point, and coordinates (x_I, y_I) and (x_O, y_O) are the coordinates of the entry point and exit point of the aircraft in the target airspace, respectively. t_I and t_O are their corresponding CTAs, and $V_{\max}$ is the maximum true airspeed of the aircraft:

CTA 约束。飞机到达目标空域的入口和出口点的时间需要满足 CTA 约束。为了使解决方案易于理解并确保每架飞机最多经历一次改航，我们在时间地理学中使用了空间-时间棱镜理论 (Miller, 1991; Klomp 等人，2015, 2019)。基于 CTA 的空间-时间棱镜模型可以推导出飞机的潜在改航路径存在于特定的椭圆形空间-时间可达区域内。考虑到假设 (a)，这个约束可以从二维角度构建。网格坐标 (X, Y) 是决策变量，坐标 (x, y) 是改航点的坐标，坐标 (x_I, y_I) 和 (x_O, y_O) 分别是飞机在目标空域的入口点和出口点的坐标。t_I 和 t_O 是它们对应的 CTA，$V_{\max}$ 是飞机的最大真实空速:

$$l_1 + l_2 \leq V_{\max} \Delta t \tag{34}$$

$$l_1 = \sqrt{(x - x_I)^2 + (y - y_I)^2} \tag{35}$$

$$l_2 = \sqrt{(x - x_O)^2 + (y - y_O)^2} \tag{36}$$

$$\Delta t = t_O - t_I \tag{37}$$

$$x = x_0 + XL + \frac{L}{2} \tag{38}$$

$$y = y_0 + YL + \frac{L}{2} \tag{39}$$

Among them, l_1 represents the distance from entry point (x_I, y_I) to rerouting point(x, y)(showed by (35)), l_2 represents the distance from rerouting point(x, y)to exit point (x_O, y_O) (showed by (36)), and δt represents the flight time of the aircraft in the airspace (showed by (37)). (38) and (39) show how to calculate the coordinates of rerouting point by the grid coordinates where it is located. Base on these, (34) means that the flight distance of the aircraft after rerouting shall not be greater than the maximum distance that the aircraft can fly in the airspace when it meets its CTA requirement. Therefore, we can determine that a feasible rerouting point is in an ellipse (Fig. 5), which can be represented by (40), where a, b, c and l_3 are given by (41),(42),(43) and (44) respectively:

其中，l_1 表示入口点 (x_I, y_I) 到重定向点 (x, y)(如图 (35) 所示) 的距离，l_2 表示重定向点 (x, y) 到出口点 (x_O, y_O) (如图 (36) 所示) 的距离，δt 表示飞机在空域中的飞行时间 (如图 (37) 所示)。(38) 和 (39) 展示

了如何通过重定向点所在的网格坐标计算重定向点的坐标。基于这些，(34) 表示飞机重定向后的飞行距离不得大于飞机在满足其 CTA 要求时在空域中可以飞行的最大距离。因此，我们可以确定一个可行的重定向点位于一个椭圆内 (图 5)，该椭圆可以表示为 (40)，其中 a, b, c 和 l_3 分别由 (41)、(42)、(43) 和 (44) 给出:

$$\frac{x^2}{a^2} + \frac{y^2}{b^2} = c^2 \tag{40}$$

$$a = \frac{1}{2} V_{\max} \Delta t \tag{41}$$

$$b = \frac{1}{2} \sqrt{a^2 - c^2} \tag{42}$$

$$c = \frac{1}{2} l_3 \tag{43}$$

$$l_3 = \sqrt{(x_O - x_I)^2 + (y_O - y_I)^2} \tag{44}$$

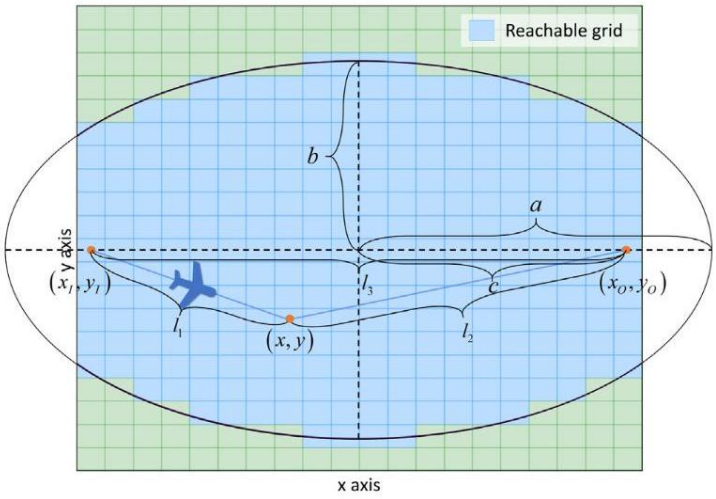

Fig. 5. Reachable solution space representation based on space-time prism.

图 5. 基于时空棱镜的可到达解空间表示。

If no rerouting points satisfy all the constraints, the adaptive CTA adjustment strategy is adopted, that is, the CTA of the aircraft in the target airspace entry point and exit point is appropriately adjusted. Generally, we postpone the CTA of the exit point. Through adjustment, the time Δt is increased by a time segment T as shown in (45), where $\Delta t'$ is the adjusted flight time of the aircraft in the target airspace:

如果没有重定向点满足所有约束，则采用自适应 CTA 调整策略，即适当调整目标空域入口点和出口点的飞机 CTA。通常，我们将出口点的 CTA 延迟。通过调整，时间 Δt 增加了一个时间段 T，如图 (45) 所示，其中 $\Delta t'$ 是飞机在目标空域的调整后飞行时间:

$$\Delta t' = \Delta t + T \tag{45}$$

(40)-(44) show that when the time Δt increases, the area of the ellipse increases. At the same time, and compared with before the adjustment, the flight's true airspeed based on the same rerouting point also changes. This means that the space-time relationship of the aircraft in the airspace changes as well. Therefore, the search space becomes larger. If a feasible solution still cannot be found at this time, the CTA is adjusted continually until there is a solution. This method is called the adaptive postponing CTA mechanism.

(40)-(44) 显示，当时间 Δt 增加，椭圆的面积也随之增加。与此同时，与调整前相比，基于相同改航点的飞行真实空速也发生了变化。这意味着飞机在空域中的时空关系也发生了变化。因此，搜索空间变得更大。如果此时仍然找不到可行解，则继续调整 CTA，直到有解为止。这种方法被称为自适应延迟 CTA 机制。

Flight conflict constraint. To ensure that there are no collisions between aircraft in the airspace, the aircraft must maintain a distance not less than the minimum separation from any other aircraft at any time. To facilitate the distinction, we call the aircraft currently undergoing optimisation decision-making the decision-making aircraft.

飞行冲突约束。为确保飞机在空域中不发生碰撞，飞机必须始终保持不小于最小间隔距离与其他任何飞机的距离。为了便于区分，我们将当前正在进行优化决策的飞机称为决策飞机。

Case 1 (without changing flight level): When the aircraft does not need to change its flight level, the constraint can be expressed by Eq. (46):

情况 1(不改变飞行高度): 当飞机不需要改变飞行高度时，该约束可以表示为方程 (46):

$$\min s_{cr,i}(x,y) \geq S_{\min}, i \in I_Z, Z = Z_{\text{initial}} \tag{46}$$

where $\min s_{cr,i}(x,y)$ is the minimum plane distance between the decision-making aircraft and aircraft i when the decision-making aircraft is cruising and coordinate(x, y)is selected as its rerouting point, $S_{\min}$ is the minimum separation in the airspace, and I_Z is the set of aircraft that exist in flight level Z of the airspace at the same time as the decision-making aircraft. It should be noted that, according to the kinematics, the distance between two objects moving in a uniform straight line in the 2D plane is a quadratic function of time, and the minimum distance between them can be obtained easily by solving the extreme value of the quadratic function in the domain of definition. Therefore, this will not be repeated in this paper.

其中 $\min s_{cr,i}(x,y)$ 是决策飞机在巡航时与飞机 i 之间的最小平面距离，当坐标 (x, y) 被选为其改航点时，$S_{\min}$ 是空域中的最小间隔距离，I_Z 是与决策飞机同时存在于空域中同一飞行高度 Z 的飞机集合。需要注意的是，根据动力学，两个在二维平面上做匀速直线运动的物体之间的距离是时间的二次函数，它们之间的最小距离可以通过求解定义域内的二次函数极值轻松得到。因此，本文不再赘述。

Case 2 (with changing flight level): If the aircraft has no feasible rerouting points without changing its flight level, the aircraft will change its flight level to expand the search space. In actual operations, the aircraft that is changing its flight level will be subject to stricter separation constraints to ensure flight safety. The controller often considers its relative position with other aircraft, flight direction, flight speed, and many other factors. To enable the autonomous operating system to determine the feasibility of climb/descent trajectories more efficiently, a novel conflict judgement model is proposed. Considering that the safety constraint between aircraft in the same flight level is the minimum safety separation when the aircraft is climbing/descending, it is required to maintain minimum safety separation with all the other aircraft in three flight levels, which are the current flight level of the aircraft, the target flight level, and the flight level between them (Fig. 6). Therefore, considering assumptions (h), (i), and (j), the constraints can be expressed as

案例二 (改变飞行高度): 如果飞机在不改变飞行高度的情况下没有可行的改航点，飞机将改变其飞行高度以扩大搜索空间。在实际操作中，改变飞行高度的飞机将受到更严格的分离约束以确保飞行安全。管制员通常会考虑与其他飞机的相对位置、飞行方向、飞行速度等诸多因素。为了使自主操作系统更有效地确定爬升/下降轨迹的可行性，提出了一个新的冲突判断模型。考虑到同一飞行高度的飞机之间的安全约束是飞机在爬升/下降时的最小安全间隔，需要与所有其他飞机在三个飞行高度上保持最小安全间隔，这三个飞行高度分别是飞机的当前飞行高度、目标飞行高度以及它们之间的飞行高度 (图 6)。因此，在考虑假设 (h)、(i) 和 (j) 的情况下，约束可以表示为

$$\min s_{cli,i}(x,y) \geq S_{\min}, i \in I_{Z_{\text{initial}}} \cup I_{(Z_{\text{initial}}+Z)/2} \cup I_Z, Z \neq Z_{\text{initial}} \tag{47}$$

$$\min s_{\text{des},i}(x,y) \geq S_{\min}, i \in I_{Z_{\text{initial}}} \cup I_{(Z_{\text{initial}}+Z)/2} \cup I_Z, Z \neq Z_{\text{initial}} \tag{48}$$

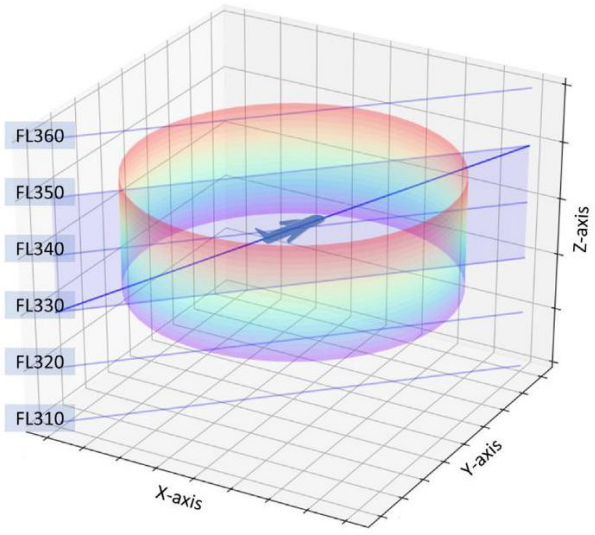

Fig. 6. Safe separation in climbing/descending process.
图 6. 爬升/下降过程中的安全间隔。

where min $s_{cli,i}(x,y)$ is the minimum plane distance between the decision-making aircraft and aircraft i when the decision-making aircraft is cruising and coordinate(x, y)is selected as its rerouting point, and min $s_{des,i}(x,y)$ is that during descent.

其中 min $s_{cli,i}(x,y)$ 是决策飞机在巡航时与飞机 i 之间的最小平面距离，坐标 (x, y) 被选为其改航点，min $s_{des,i}(x,y)$ 是在下降过程中的距离。

Restricted area constraint. To avoid the danger caused by the aircraft entering the restricted area, the trajectory is not allowed to cross the unavailable grids. Therefore, the constraint can be expressed by (49) where $V_{(x_I,y_I),(x_O,y_O)}$ is a set of coordinate points in the airspace that can establish visual paths with (x_I,y_I) and (x_O,y_O) :

限制区域约束。为了避免飞机进入限制区域带来的危险，轨迹不允许穿过不可用的格子。因此，约束可以表示为 (49)，其中 $V_{(x_I,y_I),(x_O,y_O)}$ 是一组在空域中能与 (x_I,y_I) 和 (x_O,y_O) 建立视线路径的坐标点集:

$$(x,y) \in V_{(x_I,y_I),(x_O,y_O)} \tag{49}$$

Turning angle constraint. Due to the limitations of the aircraft manoeuvrability, the turning angle of each manoeuvre of the aircraft should be less than the maximum turning angle. According to the basic knowledge of plane geometry (the function of triangle interior angle summation theorem and the function of triangle exterior angle theorem), it is only necessary for the yaw angle to satisfy the maximum turning angle constraint. Therefore, the constraint can be expressed by (50) where $\alpha_{\max}$ is the maximum turning angle corresponding to the aircraft:

转弯角度约束。由于飞机机动性的限制，飞机每次机动时的转弯角度应小于最大转弯角度。根据平面几何的基本知识 (三角形内角和定理和三角形外角定理的功能)，只需要偏航角满足最大转弯角度的约束。因此，该约束可以表示为 (50)，其中 $\alpha_{\max}$ 是对应于飞机的最大转弯角度:

$$\pi - \arccos\left(\frac{{l_1}^2 + {l_2}^2 - {l_3}^2}{2l_1 l_2}\right) \leq \alpha_{\max} \tag{50}$$

True airspeed constraint. Due to the limitation of aircraft flight performance, the true airspeed of the aircraft should be within the allowable speed range.

真空速约束。由于飞机飞行性能的限制，飞机的真空速应在允许的速度范围内。

Case 1 (without changing flight level): In this condition, the constraint can be expressed by (51) and (52), respectively. where $V_{cr,Z,\min}$ and $V_{cr,Z,\max}$ are the minimum and maximum cruise speeds of the aircraft at flight level Z , respectively:

情况 1(不改变飞行高度): 在这种情况下，约束可以分别表示为 (51) 和 (52)。其中 $V_{cr,Z,\min}$ 和 $V_{cr,Z,\max}$ 分别是飞机在飞行高度 Z 下的最小和最大巡航速度:

$$v \in [V_{cr,Z,\min}, V_{cr,Z,\max}] \tag{51}$$

$$v = \frac{l_1 + l_2}{\Delta t} \tag{52}$$

Case 2 (with changing flight level): Under this condition, the constraints can be expressed by (53), (54) and (55):

情况 2(改变飞行高度): 在这种情况下，约束可以表示为 (53)、(54) 和 (55):

$$v \in [V_{cr,Z_{\text{initial}},\min}, V_{cr,Z_{\text{initial}},\max}] \tag{53}$$

$$v \in [V_{cli,Z,\min}, V_{cli,Z,\max}] \cap [V_{cli,Z_{\text{initial}},\min}, V_{cli,Z_{\text{initial}},\max}] \tag{54}$$

$$v \in [V_{des,Z,\min}, V_{des,Z,\max}] \cap [V_{des,Z_{\text{initial}},\min}, V_{des,Z_{\text{initial}},\max}] \tag{55}$$

Among them, the meanings of the types of V are similar to $V_{cr,Z,\min}$ and $V_{cr,Z,\max}$ and readers can easily get their exact meaning through their subscripts.

其中，V 类型的含义与 $V_{cr,Z,\min}$ 和 $V_{cr,Z,\max}$ 类似，读者可以通过它们的下标轻松理解它们的准确含义。

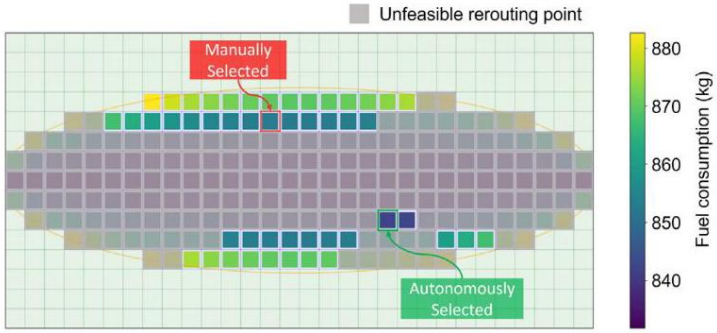

Fig. 7. Rerouting cost distribution in reachable solution space.
图 7. 可达解空间中的重新路由成本分布。

5.2.5. Algorithm design

5.2.5. 算法设计

Because this optimisation model is a nonlinear integer programming problem, which is difficult to solve using a precise algorithm, a heuristic algorithm is often used to solve it. However, the model only includes three decision variables, namely X, Y and Z . Moreover, the number of potential rerouting grids to be searched is very limited when the grid size is not very small, so the enumeration method was adopted to traverse and search all potential rerouting grids. In terms of safety, the enumeration method is the safest method (Landry et al., 2010). Through the above constraints, the feasible rerouting grid is screened out, and the optimal rerouting grid is selected to obtain the optimal rerouting point and the corresponding trajectory. It should be further explained that the enumeration method is designed to realise the solution space visualisation. In other words, the algorithm generates the reachable solution space and its cost distribution based on the performance expectations of the AU and ATM. Controllers and pilots can intuitively understand the safety and reasonableness of the rerouting trajectory provided by the algorithm through a human-machine interface. From this perspective, the solution space visualisation of our method has the potential to support effective human-machine interaction. Besides, in some cases more decision-making information can be provided for controllers and pilots (such as when they need to manually select a non-optimal rerouting point). For example, Fig. 7 shows the rerouting cost distribution in reachable solution space where we can see the feasibility and fuel consumption of each potential rerouting grid. If the decision-makers think the optimal rerouting point has a higher risk due to its very small manoeuvre space, they can choose another rerouting point that they think is more suitable based on the human-machine interaction interface. Assuming that it was the controller that proposed the above changes, the pilots were able to intuitively understand the controller's motivation and vice versa. From this perspective, the solution space visualisation of our method has the potential to support air-ground coordination also.

由于这个优化模型是一个非线性整数规划问题，使用精确算法求解较为困难，因此通常使用启发式算法来求解。然而，模型仅包括三个决策变量，即 X, Y 和 Z 。此外，当网格大小不太小时，需要搜索的潜在重路由网格数量非常有限，因此采用了枚举方法来遍历和搜索所有潜在的重路由网格。在安全性方面，枚举方法是最安全的方法 (Landry et al., 2010)。通过上述约束，筛选出可行的重路由网格，并选择最优重路由网格以获得最优重路由点和相应的轨迹。需要进一步解释的是，枚举方法旨在实现解空间的可视化。换句话说，算法根据 AU 和 ATM 的性能预期生成可达解空间及其成本分布。通过人机界面，管制员和飞行员可以直观地理解算法提供的重路由轨迹的安全性和合理性。从这个角度来看，我们的方法的解空间可视化有潜力支持有效的人机交互。此外，在某些情况下，可以为管制员和飞行员提供更多的决策信息 (例如，当他们需要手动选择一个非最优重路由点时)。例如，图 7 显示了可达解空间中的重路由成本分布，我们可以看到每个潜在重路由网格的可行性和燃油消耗。如果决策者认为最优重路由点由于其非常小的机动空间而具有更高的风险，他们可以根据人机交互界面选择他们认为更合适的另一个重路由点。假设是管制员提出了上述变更，飞行员能够直观地理解管制员的动机，反之亦然。从这个角度来看，我们的方法的解空间可视化也有潜力支持空地协调。

The autonomous re-planning of the optimal agreed trajectory method is shown in Algorithm 2. For an aircraft about to enter the airspace, the agreed trajectories of an aircraft currently in the airspace and the real-time airspace information are inputted first. Next, if the desired trajectory of the aircraft is conflict-free with other agreed trajectories, the desired trajectory of the aircraft will be taken as the agreed trajectory (lines 3 and 4). Otherwise, the reachable area of the aircraft will be calculated by the space-time prism based on the CTA and all feasible rerouting

trajectories without changing the flight level are found where the optimal one will be taken as the agreed trajectory of the aircraft (lines 6-9). However, if none are found, search feasible rerouting trajectories with a changing flight level and take the optimal one as the agreed trajectory of the aircraft (lines 11-13). If none are still found, the adaptive postponing CTA mechanism will be activated, that is, the CTA of the aircraft's exit point will be postponed (line 19) and the above steps will be repeated until the agreed trajectory is achieved (lines 2-19). Finally, the agreed trajectory of the aircraft is outputted.

自主重新规划最优协商轨迹的方法如算法 2 所示。对于即将进入空域的飞机，首先输入当前在空域中的飞机的协商轨迹和实时空域信息。接下来，如果飞机期望的轨迹与其他协商轨迹无冲突，则该飞机的期望轨迹将被作为协商轨迹 (第 3 和第 4 行)。否则，根据 CTA 和所有不改变飞行高度的可行重路由轨迹，利用空间时间棱镜计算飞机的可达区域，并找到最优轨迹作为飞机的协商轨迹 (第 6-9 行)。如果没有找到，搜索可行且改变飞行高度的重路由轨迹，并将最优轨迹作为飞机的协商轨迹 (第 11-13 行)。如果仍然没有找到，将激活自适应延迟 CTA 机制，即延迟飞机退出点的 CTA(第 19 行)，并重复上述步骤直到获得协商轨迹 (第 2-19 行)。最后，输出飞机的协商轨迹。

It is expected that the conflict-free-trajectory real-time re-planning based on the space-time reachable area of a flight trajectory cannot only support the autonomous trajectory operation in the FRA but can also provide consistent situational awareness as well as a transparent and friendly human-machine interface. Especially for special situations, controllers or pilots can safely and seamlessly take over airspace or aircraft operation, effectively reducing the potential risk of autonomous operation.

预期基于航班轨迹的空间时间可达区域的冲突自由轨迹实时重规划不仅能支持 FRA 中的自主轨迹运行，还能提供一致的情况意识，以及透明友好的人机界面。特别是在特殊情况下，管制员或飞行员可以安全无缝地接管空域或飞机操作，有效降低自主操作潜在的风险。

6. Case study

6. 案例研究

In this section, we designed a high-density simulation scenario with a restricted area and multiple flight levels to validate the effectiveness, efficiency, stability, and timeliness of the proposed method. The case study was carried out on a customised simulator. The simulation is divided into four parts: airspace parameterisation, agreed trajectory (strategic) generation, desired trajectory (pre-planning) generation and agreed trajectory (tactical) generation, and they correspond to the four modules in the operational framework. The computer processor used in this simulation was an Intel(R) Core (TM) i7-10510U CPU @ 1.80 Hz 2.30 GHz and the programming language was Python 3.

在本节中，我们设计了一个具有限制区域和多飞行级别的高密度仿真场景，以验证所提出方法的有效性、效率、稳定性和及时性。案例研究是在一个定制的模拟器上进行的。仿真分为四个部分: 空域参数化、协议轨迹 (战略) 生成、期望轨迹 (预规划) 生成和协议轨迹 (战术) 生成，它们对应于操作框架中的四个模块。本次仿真所使用的计算机处理器是 Intel(R) Core(TM) i7-10510U CPU @ 1.80 Hz 2.30 GHz，编程语言为 Python 3。

Algorithm 2 Autonomous re-planning of the optimal agreed trajectory Input: the desired trajectory of the aircraft trajectory y_{desired} , agreed trajectories of other aircraft, airspace condition

1: initialise the agreed trajectory of the aircraft trajectory $_{\text{agreed}}$ and the set of feasible rerouting trajectories $TRAJECTORY_{\text{feasible}}$

while trajectory $_{\text{agreed}}$ is null do

if trajectory y_{desired} is conflict-free with trajectories of other aircraft then

trajectory $_{\text{agreed}} \leftarrow$ trajectory $_{\text{desired}}$

else

generate reachable area of the aircraft by the space-time prism based on the CTA

search the feasible rerouting trajectories in the reachable area of the current flight level and form $TRAJECTORY_{\text{feasible}}$

if $TRAJECTORY_{\text{feasible}}$ is not null then

take the optimal trajectory in TRAJECTORY $_{\text{feasible}}$ as trajectory $_{\text{agreed}}$

else

search feasible rerouting trajectories in the reachable area of the adjacent flight levels with the same direction and form

TRAJECTORY $_{\text{feasible}}$

if $TRAJECTORY_{\text{feasible}}$ is not null then

take the optimal trajectory in TRAJECTORY $_{\text{feasible}}$ as trajectory $_{\text{agreed}}$

else

activate the adaptive postponing CTA mechanism (postpone the CTA)
end if
end if
end if
end while
Jutput: trajectory agreed

6.1. Simulation scenarios

6.1. 仿真场景

In the current real world, there is no sector where the air traffic flow can be very large, such as 500 per hour or more, when there are restricted areas in it. And, as far as we know, few similar experiments with such high-density scenario have been reported. Moreover, on this basis, the similar study considering human-machine interaction is rarely reported. Therefore, the scenario and function of the framework proposed in this paper are original to some extent and a simulated airspace was designed. Simulation data were generated to verify the performance of the model and algorithm. We constructed a simulated airspace with dimensions of 300 km $\times$ 300 km $\times$ 6 FL (shown as Fig. 8). There were four entry points and four exit points in each flight level. To be consistent with the actual operating situation, the flight direction of the odd-numbered flight levels was opposite to that of the even-numbered flight level. Based on the operating concept of the TBO, several conflict-free agreed trajectories of Boeing 737-800 aircraft were randomly generated. All the aircraft operating parameters came from BADA (EUROCONTROL, 2010). The time when these aircraft entered the airspace was evenly distributed in one hour, as presented in (56), where t_{interval} is the time interval for the aircraft to enter the airspace, and n_{flow} is the air traffic flow per hour:

在当前现实世界中，没有任何一个领域的空中交通流量可以非常大，例如每小时 500 次或更多，同时其中有限制区域。据我们所知，很少有类似的高密度场景的实验报道。此外，在此基础上，考虑人机交互的类似研究也鲜有报道。因此，本文提出的框架的场景和功能在一定程度上是原创的，并设计了一个模拟的空域。生成模拟数据以验证模型和算法的性能。我们构建了一个尺寸为 300 km $\times$ 300 km $\times$ 6 FL (如图 8 所示) 的模拟空域。在每一个飞行高度层有四个入口点和四个出口点。为了与实际运行情况保持一致，奇数飞行高度的飞行方向与偶数飞行高度相反。基于 TBO 的运行理念，随机生成了几条波音 737-800 飞机的无冲突协议轨迹。所有飞机的运行参数均来自 BADA(EUROCONTROL，2010)。这些飞机进入空域的时间在一小时内均匀分布，如 (56) 所示，其中 t_{interval} 是飞机进入空域的时间间隔，n_{flow} 是每小时空中交通流量:

$$t_{\text{interval}} = \frac{1}{n_{\text{flow}}} \tag{56}$$

Considering the actual operation rules, we set the minimum horizontal safety interval of the aircraft to 10 km and the plane grid side length to the same value. In the kinematics model, we assumed that the state of motion was instantaneous. Thus, to make the simulation more realistic, we further assumed that the maximum turning angle of the aircraft was 60°.

考虑实际运行规则，我们将飞机的最小水平安全间隔设置为 10 km，并将飞机网格边长设置为相同的值。在动力学模型中，我们假设运动状态是瞬时的。因此，为了使模拟更加真实，我们进一步假设飞机的最大转弯角度为 60°。

We generated 10 flight plan samples for eight conditions of traffic flow per hour: 100, 200, 300, 400, 500, 600, 700, and 800 aircraft per hour, that is, 80 samples in total. An restricted area was set up in the centre of the airspace. The resulting unavailable grid formed a 60 km $\times$ 60 km $\times$ 4 FL rectangle (Fig. 9). From the desired trajectory generation model in Section 5.1, the desired trajectory depends only on the entry and exit points of the aircraft and the boundary position of the restricted area. Therefore, there were 14 types of desired trajectories in each flight level and a total of 84 types in six flight levels.

我们生成了 10 个飞行计划样本，针对每小时 100、200、300、400、500、600、700 和 800 架飞机的 8 种交通流量条件，即总共 80 个样本。在空域中心设立了一个限制区域。由此形成的不可用网格构成了 60 km $\times$ 60 km $\times$ 4 FL 矩形 (图 9)。从第 5.1 节中的期望轨迹生成模型来看，期望轨迹仅取决于飞机的入口和出口点以及限制区域的边界位置。因此，每个飞行级别有 14 种期望轨迹类型，六个飞行级别共有 84 种类型。

6.2. Results analysis

6.2. 结果分析

It should be noted that most of the methods and techniques for decision-making support based on trajectory planning are closely linked to the specific application scenarios and tasks, making any comparison of different approaches hardly objective (Wang et al., 2020). Since the proposed method in this paper is intended to solve a new trajectory planning problem considering the human-machine interaction in future TBO scenarios, and no similar studies have been reported so far, we can only attempt to demonstrate that the performance of this method is promising through a large number of tests. In view of this, based on the operating trajectory data of 80 samples (Fig. 10 shows the agreed trajectory of one of the samples with an air traffic flow rate of 600 aircraft per hour), we validated our proposed method from four aspects: effectiveness, efficiency, stability, and timeliness.

应该注意的是，大多数基于轨迹规划的决策支持方法和技术与特定的应用场景和任务紧密相关，这使得不同方法的比较很难做到客观 (Wang 等人，2020 年)。由于本文提出的方法旨在解决未来 TBO 场景中考虑人机交互的新轨迹规划问题，且迄今为止尚未有类似研究报道，因此我们只能通过大量测试来尝试证明这种方法的表现是有前景的。基于此，根据 80 个样本的运行轨迹数据 (图 10 显示了其中一个样本在每小时 600 架飞机的空中交通流量下的同意轨迹)，我们从四个方面验证了我们提出的方法: 有效性、效率、稳定性和及时性。

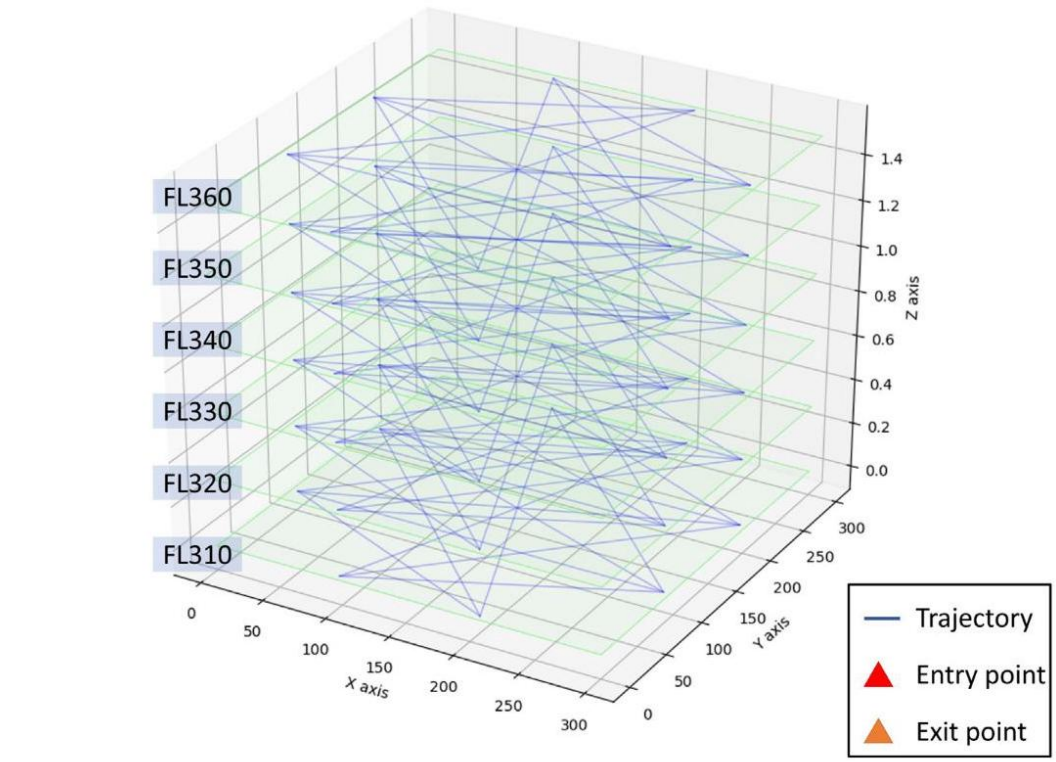

(a) 3D View

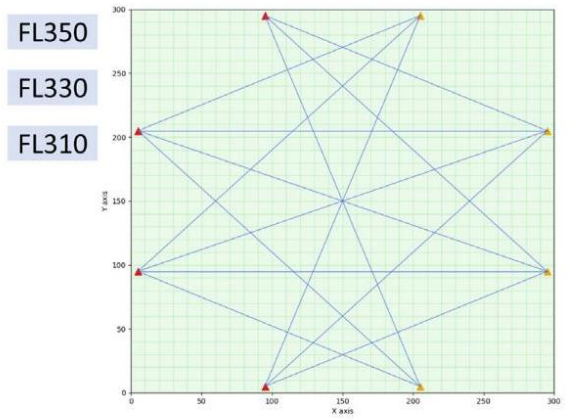

(b) 2D View of Odd Flight Levels

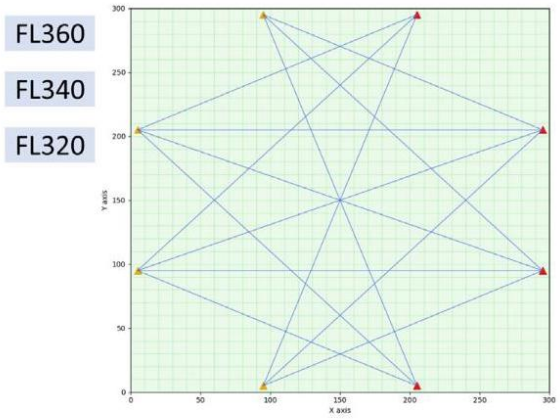

(c) 2D View of Even Flight Levels

Fig. 8. Agreed trajectory (strategic).

图 8. 同意轨迹 (战略)。

The four performance metrics used here are effectiveness, efficiency, stability and timeliness. They are described as follows. Effectiveness refers to the ability to resolve potential conflicts in real-time operation. This is the most important safety index for evaluating a conflict resolution algorithm. As for efficiency, it refers to the extra flight cost caused by trajectory planning algorithms. In this paper, it mainly includes the extra flight distance, flight delays, and extra fuel consumption. Stability refers to the domino effect produced when an initial conflict is resolved. In high-density traffic scenarios, CR often leads to secondary conflicts, namely, the domino effect, which is an important index to measure the stability of the CR algorithm. The weaker the domino effect is, the more stable the algorithm becomes. Finally, timeliness refers to the computing efficiency in generating conflict-free trajectories. This is one of the key performance metrics to determine whether the proposed algorithms run fast enough for real-time operation.

在此处使用的四个性能指标是有效性、效率、稳定性和及时性。它们描述如下。有效性指的是在实时

操作中解决潜在冲突的能力。这是评估冲突解决算法最重要的安全指标。至于效率，它指的是由轨迹规划算法引起的额外飞行成本。在本文中，它主要包括额外的飞行距离、飞行延误和额外燃油消耗。稳定性指的是解决初始冲突时产生的多米诺效应。在高度密集的流量场景中，冲突解决 (CR) 经常导致次生冲突，即多米诺效应，这是衡量 CR 算法稳定性的重要指标。多米诺效应越弱，算法越稳定。最后，及时性指的是生成无冲突轨迹的计算效率。这是确定所提出算法是否足够快速以适应实时操作的关键性能指标之一。

6.2.1. Effectiveness

6.2.1. 有效性

Fig. 11 shows the relevant results in terms of the effectiveness. Among them, if an aircraft fails to operate on the desired trajectory during real-time operation, it is recorded as a potential conflict. We classify potential conflicts into minor and major potential conflicts.

图 11 显示了关于有效性的相关结果。其中，如果在实时操作中飞机未能按照期望的轨迹运行，则记录为潜在冲突。我们将潜在冲突分为小冲突和重大潜在冲突。

If a potential conflict can be resolved only by delaying the CTA in five units of time at the exit point (where 1 unit of time is 20 s), we call it a minor potential conflict; otherwise, it is a major potential conflict. It should be noted that, although a major potential

如果潜在冲突只能通过在出口点延迟 CTA 五个时间单位 (其中 1 个时间单位为 20 秒) 来解决，我们称之为小冲突；否则，它是重大潜在冲突。应注意，尽管重大冲突不能仅通过在出口点延迟 CTA 五个时间单位来解决，但它可以通过其他方式解决，例如通过调整入口点的 CTA、等待以及其他可行的战术机动。

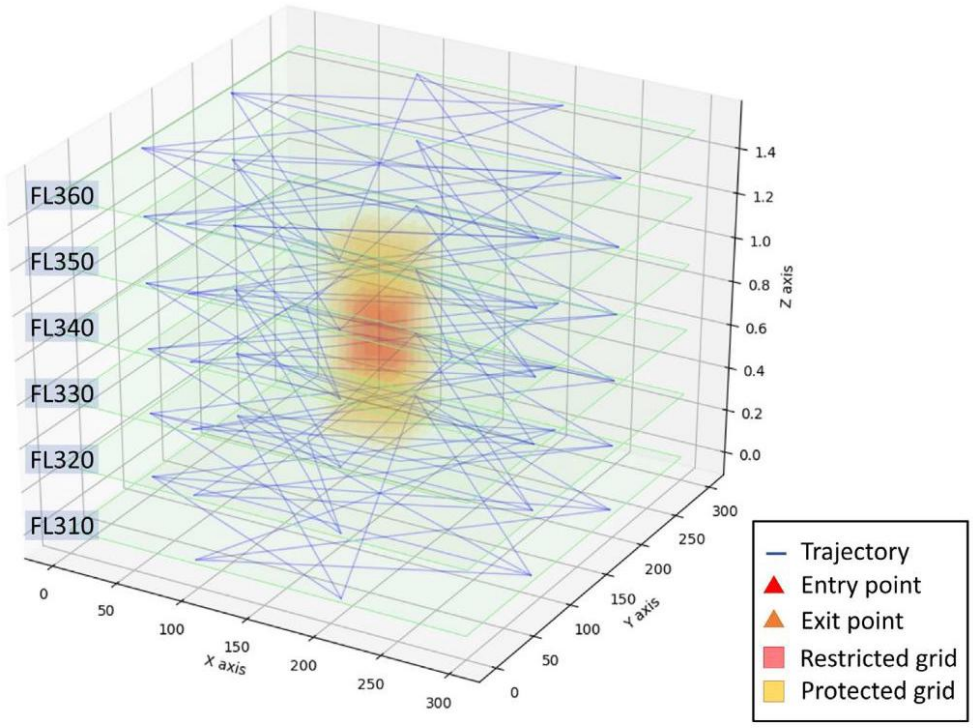

(a) 3D View

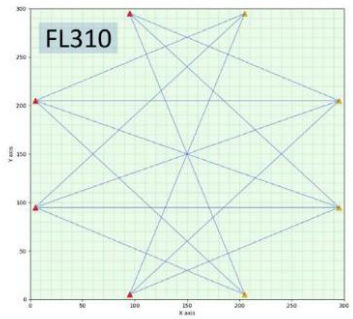

(b) 2D Top View of FL310

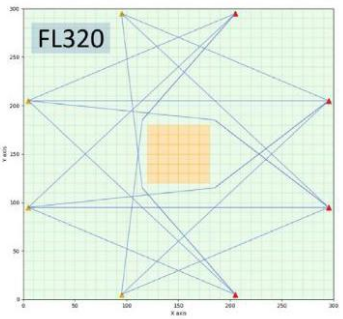

(c) 2D Top View of FL320

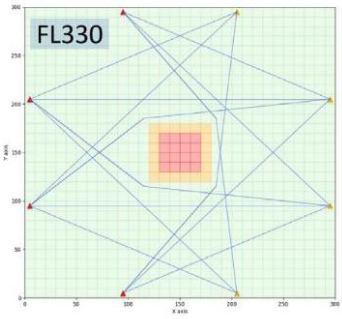

(d) 2D Top View of FL330

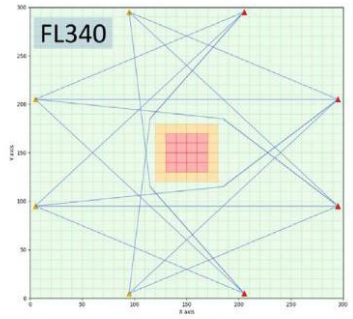

(e) 2D Top View of FL340

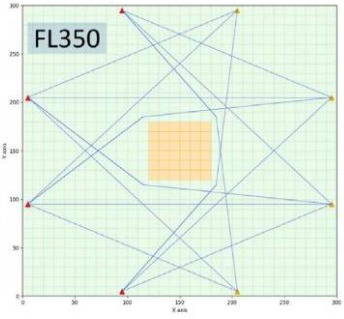

(f) 2D Top View of FL350

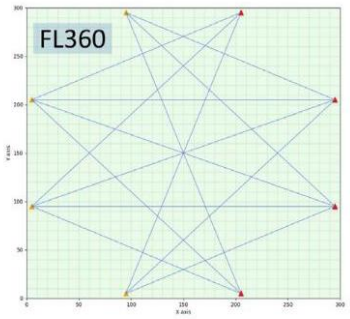

(g) 2D Top View of FL360

Fig. 9. Desired trajectory before entering the sector.

图 9. 进入扇区前的期望轨迹。

conflict cannot be resolved only by delaying the CTA in five units of time at the exit point, it can be resolved in other ways, such as by adjusting the CTA of the entry points, holding, and other feasible tactical manoeuvres.

冲突不能仅通过在出口点延迟 CTA 五个时间单位来解决，但它可以通过其他方式解决，例如通过调整入口点的 CTA、等待和其他可行的战术机动。

Based on simulation data, we believe that a reasonable threshold of the air traffic flow in this airspace is the maximum air traffic flow when the number of major potential conflicts is zero. Therefore, 600 aircraft is the threshold of the air traffic flow per hour in this airspace. In other words, the algorithm can resolve all conflicts in a 300 km × 300 km × 6FL simulated airspace with a 60 km × 60km × 4FL restricted area with no more than 600 aircraft per hour, which shows that the algorithm is effective in resolving conflicts in the multi-flight level airspace with a restricted area.

基于模拟数据，我们认为该空域内合理的航空流量阈值是当主要潜在冲突数量为零时的最大航空流量。因此，600 架飞机是该空域每小时航空流量的阈值。换句话说，算法可以在一个 300 km × 300 km × 6FL 模拟空域中解决所有冲突，该空域有一个 60 km × 60km × 4FL 的限制区域，每小时不超过 600 架飞机，这表明算法在解决带有受限区域的多层次航路空域冲突中是有效的。

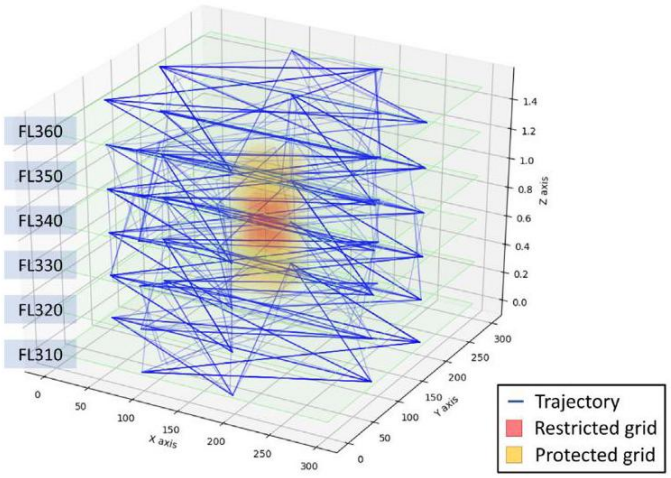

(a) 3D View

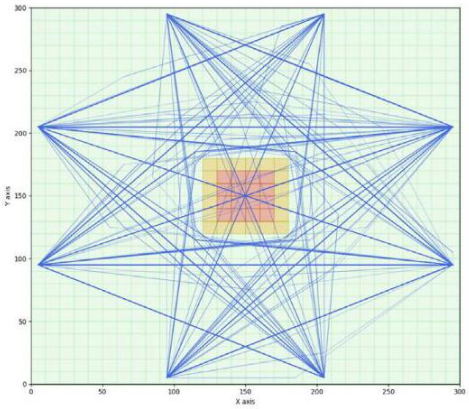

(b) 2D Top View

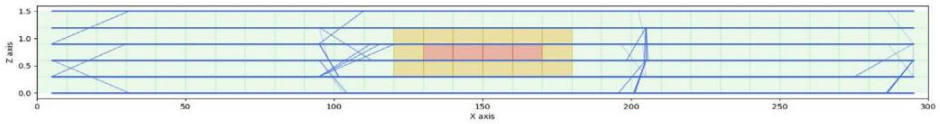

(c) 2D Side View from Y Axis

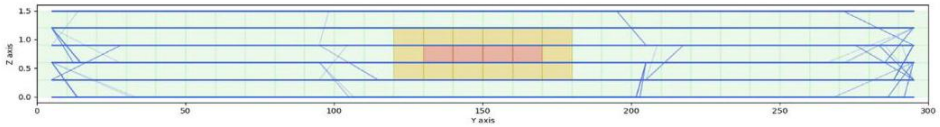

(d) 2D Side View from X Axis

Fig. 10. Agreed trajectory (tactical).

图 10. 达成轨迹 (战术)。

When the air traffic flow exceeds this threshold, major potential conflicts will increase dramatically. In addition, the number of potential conflicts increases with the growth of the air traffic flow, and the rate of potential conflicts grows almost linearly. This indicates that with the increase in the airspace traffic density, potential conflicts emerge more frequently, and the number of conflicts shows an exponential growth trend.

当航空流量超过这个阈值时，主要潜在冲突将急剧增加。此外，潜在冲突的数量随着航空流量的增加而增加，潜在冲突的增长率几乎呈线性增长。这表明随着空域交通密度的增加，潜在冲突更频繁地出现，冲突的数量呈现指数增长趋势。

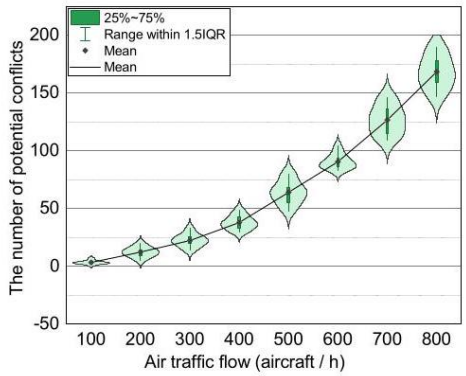

(a) The number of potential conflicts

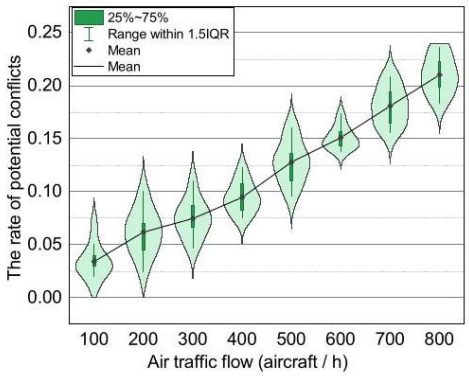

(b) The rate of potential conflicts

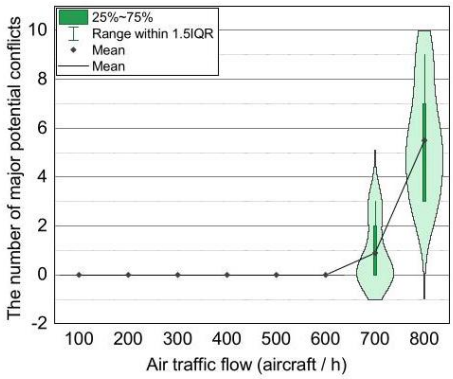

(c) The number of major potential conflicts

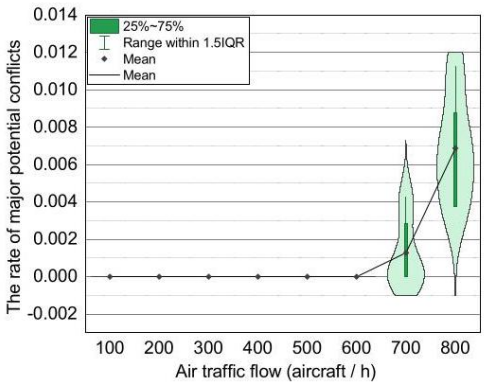

(d) The rate of major potential conflicts

Fig. 11. Flight conflict evolution with demand.

图 11. 随着需求的航班冲突演变。

From the rate of potential conflicts, most of the desired trajectories were eventually accepted as agreed trajectories. This in a way implies that the trajectory pre-planning plays an active role in reducing the amount of computation required for real-time trajectory planning.

从潜在冲突率来看，最终大多数期望轨迹被接受为达成轨迹。这在某种程度上意味着轨迹预规划在减少实时轨迹规划所需的计算量方面发挥了积极作用。

6.2.2. Efficiency

6.2.2. 效率

Fig. 12 shows the extra flight cost evolution. The extra flight cost refers to the increased cost of an agreed trajectory compared to a desired trajectory. Consistent with the variation trends of the conflicts, the three efficiency indices all showed accelerated growth with the increase in the air traffic flow. When the air traffic flow per hour in this airspace was less than the threshold (600 aircraft, as mentioned previously), the average extra flight distance, average flight delay, and average extra fuel consumption were less than 0.41 km, 2.1 s , and 1.5 kg , respectively, which were almost negligible compared with the actual operation.

图 12 显示了额外飞行成本的演变。额外飞行成本是指达成轨迹相较于期望轨迹增加的成本。与冲突的变化趋势一致，三个效率指标都随着航空流量的增加而呈现加速增长。当该空域每小时的航空流量低于阈值 (如前所述的 600 架飞机) 时，平均额外飞行距离、平均飞行延误和平均额外燃油消耗均小于 0.41 km, 2.1 s 和 1.5 kg ，与实际运行相比几乎可以忽略不计。

Fig. 13 shows the relationship between different flight costs. With the growth of air traffic flow per hour in this airspace, when it was less than the threshold, the growth rates of extra fuel consumption and extra flight distance were much faster than that of extra flight delay and the gap was gradually narrowing. This is because when the traffic density in airspace was low, the aircraft rerouting distance was relatively short, and the delay can be avoided to a great extent by accelerating. However, with the increase of airspace density, flight conflict emerged rapidly. Aircraft needed to rerouting for a longer distance to avoid conflict and acceleration was not enough to avoid delay. When the air traffic flow per hour was more than the threshold, the airspace traffic situation became less ordered, the rerouting distance of aircraft was close to the limit, and more aircraft had to delay for a long time. Therefore, extra flight delay became the major extra cost at this time. Moreover, the growth rate of extra fuel consumption is similar to that of extra flight distance. The reason is that with the increase of airspace density, aircraft rerouting distance increased to avoid more complex conflicts, and when the acceleration was not enough to eliminate the delay caused by longer flight distance, most rerouting aircraft flied at maximum speed. Therefore, in this case, the extra flight distance became the determinant of the extra fuel consumption.

图 13 显示了不同飞行成本之间的关系。随着该空域每小时空中交通流的增长，当其小于阈值时，额外燃油消耗和额外飞行距离的增长率远快于额外飞行延误，且差距逐渐缩小。这是因为当空域交通密度较低时，飞机改航距离相对较短，通过加速可以在很大程度上避免延误。然而，随着空域密度的增加，飞行冲突迅速出现。飞机需要飞更远的距离来避开冲突，加速不足以避免延误。当每小时空中交通流超过阈值时，空域交通状况变得更有序，飞机改航距离接近极限，更多飞机不得不长时间延误。因此，额外飞行延误成为此时主要的额外成本。此外，额外燃油消耗的增长率与额外飞行距离相似。原因是随着空域密度的增加，飞机改航距离增加以避免更复杂的冲突，当加速不足以消除由更长飞行距离引起的延误时，大多数改航飞机以最大速度飞行。因此，在这种情况下，额外飞行距离成为额外燃油消耗的决定因素。

Fig. 14 shows the frequency of flight level change. The trends for the extra flight distance and the extra fuel consumption were roughly the same, but interestingly, the variation trend of the number of aircraft changing flight levels also exhibited continuous growth. When the airspace flow tends to be saturated, only less than 3% aircraft changed flight levels. Thus, we can reasonably infer

图 14 显示了飞行高度变化的频率。额外飞行距离和额外燃油消耗的趋势大致相同，有趣的是，改变飞行高度的飞机数量也呈现出持续增长的趋势。当空域流量趋于饱和时，只有不到 3% 架飞机改变了飞行高度。因此，我们可以合理推断

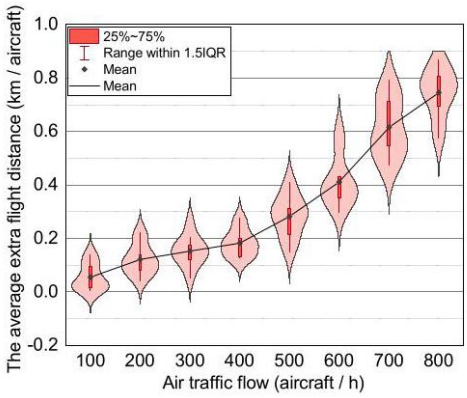

(a) The average extra flight distance

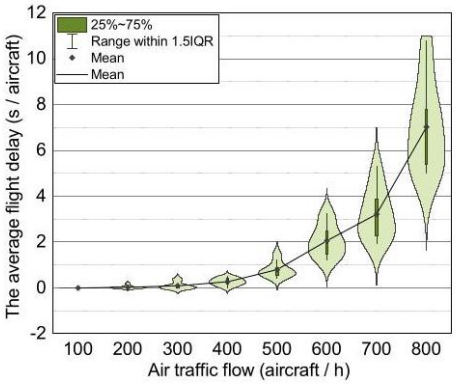

(b) The average flight delay

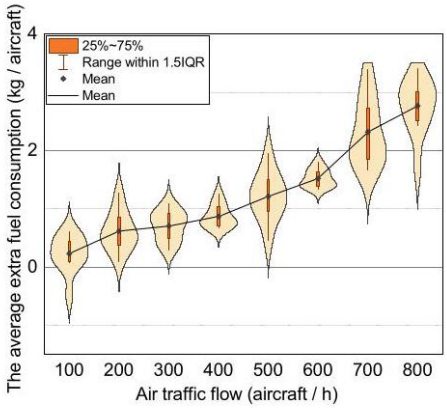

(c) The average extra fuel consumption

Fig. 12. Extra flight cost evolution.
图 12。额外飞行成本演变。

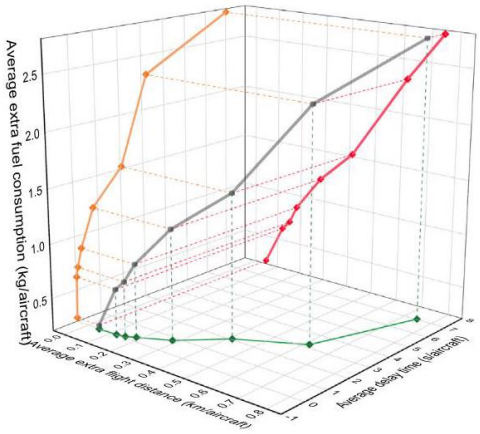

Fig. 13. Relationship between different flight costs.
图 13。不同飞行成本之间的关系。

that, in the FRA, changing the flight levels is an important method for CR. The method can effectively reduce the flight delays and not necessarily generate additional economic costs, because the aircraft can reduce fuel consumption by switching to a higher flight level. Although when the airspace flow tends to be saturated, a larger

proportion of aircraft need to effectively resolve conflicts by changing the flight altitude, this is still only a small proportion of the total aircraft.

在 FRA 中，改变飞行高度是解决冲突的重要方法。这种方法可以有效减少航班延误，并且不一定产生额外的经济成本，因为飞机通过切换到更高的飞行高度可以减少燃油消耗。尽管当空域流量趋于饱和时，较大比例的飞机需要通过改变飞行高度有效解决冲突，但这仍然只占总飞机数量的一小部分。

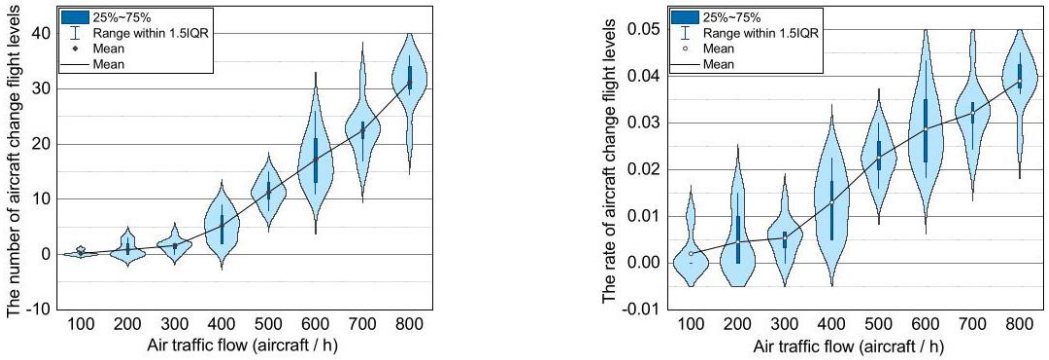

(a) The number of aircraft change flight levels

(b) The rate of aircraft change flight levels

飞行高度层

Fig. 14. Frequency of flight level change.

图 14. 飞行高度层变更频率。

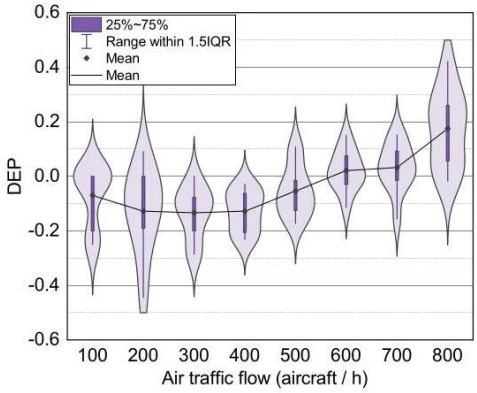

Fig. 15. Domino Effect Parameter (DEP).

图 15. 多米诺效应参数 (DEP)。

6.2.3. Stability

6.2.3. 稳定性

In terms of the principle of CR, the method in this paper uses one-to-many CR, that is, in the search for the rerouted trajectory, it is ensured that the feasible rerouted trajectory is the conflict-free trajectory of all the aircraft in the airspace, which avoids the domino effect from the CR method. In previous studies, the Domino Effect Parameter (DEP) is commonly used to characterise the degree of impact of the CR on the airspace stability (Bilimoria et al.,2000). The expression of the index I_{DEP} is given by (57), where C_1 is the number of potential conflicts in the airspace when all the aircraft are flying on the desired trajectory, and C_2 is the number of potential conflicts in the airspace when all aircraft are flying on the agreed trajectory (tactical):

在冲突解决 (CR) 原则方面，本文采用的一对多 CR 方法，即在寻找改航轨迹时，确保可行的改航轨迹是空域中所有飞机的无冲突轨迹，从而避免了 CR 方法引起的多米诺效应。在以往的研究中，多米诺效应参数 (DEP) 通常被用来表征 CR 对空域稳定性的影响程度 (Bilimoria 等人，2000 年)。该指标 I_{DEP} 的表达式由 (57) 给出，其中 C_1 是当所有飞机都按照期望轨迹飞行时空域内潜在的冲突数量，C_2 是当所有飞机都按照协议轨迹 (战术) 飞行时空域内潜在的冲突数量。

$$I_{\mathrm{DEP}} = \frac{C_1 - C_2}{C_1} = \frac{C_2}{C_1} - 1 \tag{57}$$

Fig. 15 shows the DEP in the simulation of each sample. The DEP remained below 0 until the air traffic flow in the airspace was saturated. This was because the paths of the aircraft with the same entry and exit points were the same when using the visibility graph for the desired trajectory planning. Therefore, potential conflicts in the airspace were relatively concentrated at the intersection point of the desired trajectories. When an aircraft has potential conflicts with several aircraft in succession near the same intersection point, its rerouting will largely avoid the area where the conflicts are concentrated, thus facilitating the resolution of other potential conflicts. It finally showed the effect of resolving multiple potential conflicts at one time.

图 15 显示了在每种样本的模拟中的 DEP。当空域中的空中交通流量饱和之前，DEP 保持在 0 以下。这是因为当使用可见性图进行期望轨迹规划时，具有相同进出点的飞机的路径是相同的。因此，空域中的潜在冲突相对集中在期望轨迹的交点。当一架飞机在同一个交点附近连续与几架飞机存在潜在冲突时，其重新规划将很大程度上避开冲突集中的区域，从而有助于解决其他潜在的冲突。它最终展示了在一次解决多个潜在冲突的效果。

From an overall perspective of Fig. 15, the DEP showed a trend of first decreasing and then increasing. As mentioned, our method has the advantage that it can often resolve multiple potential conflicts by a single rerouting, especially when multiple potential conflicts are near each other. When air traffic flow was very low (e.g., 100 aircraft per hour), the number of potential conflicts (C_1) was low and the spatial distribution of conflicts was scattered, making it difficult for our method to show its advantage in this scenario. As the density increased, the number of potential conflicts (C_1) got higher and their location became more concentrated, thus allowing the advantage of our method to emerge (C_2 kept low). Besides, in medium-to-low density scenarios (e.g., from 100 to 400 aircraft per hour), the secondary conflicts resulting from the rerouting were not significant. That is why the DEP decreased at the beginning. As the traffic density of airspace increased further (e.g., from 400 to 800 aircraft per hour), the number of secondary conflicts due to rerouting naturally increased rapidly, resulting in an upward trend in DEP finally (C_2 increased more rapidly than C_1), despite the advantage of our method being further exploited. Nevertheless, when the air traffic flow was less than 600 aircraft per hour, the DEP was less than 0 . This means that our CR method did not lead to a significant domino effect when the airspace was not saturated, rather, on average, the number of potential conflicts it resolved through a single rerouting was greater than the number of secondary conflicts it generated.

从图 15 的整体视角来看，DEP 呈现出先减少后增加的趋势。如前所述，我们的方法有一个优点，即通常可以通过一次重新路由来解决多个潜在的冲突，特别是在多个潜在冲突相互靠近的情况下。当空中交通流量非常低 (例如，每小时 100 架飞机) 时，潜在冲突的数量 (C_1) 较低，冲突的空间分布较为分散，这使得我们的方法在这种场景下难以显示其优势。随着密度的增加，潜在冲突的数量 (C_1) 变得更高，它们的位置变得更加集中，从而使我们的方法的优势得以显现 (C_2 保持低值)。此外，在中低密度场景下 (例如，每小时 100 到 400 架飞机)，由于重新路由产生的二次冲突并不显著。这就是为什么 DEP 一开始就下降了。随着空域交通密度的进一步增加 (例如，从 400 到 800 架飞机)，由于重新路由导致的二次冲突数量自然迅速增加，最终导致 DEP 呈现上升趋势 ((C_2 增加速度超过了 C_1)，尽管我们的方法优势得到了进一步利用。然而，当空中交通流量小于每小时 600 架飞机时，DEP 小于 0。这意味着，当空域未饱和时，我们的 CR 方法并没有导致显著的连锁反应，相反，平均而言，通过一次重新路由解决的潜在冲突数量大于它产生的二次冲突数量。

Table 3

表 3

Analysis of variance of DEP (P -value).

DEP(P -值) 的方差分析。

100	200	300	400	500	600	700	800
100	0.3584	0.1945	0.1950	0.7392	0.0489	0.0387	0.0005
200		0.9277	0.9934	0.2199	0.0147	0.0120	0.0003
300			0.9008	0.0780	0.0008	0.0009	0.0000
400				0.0685	0.0003	0.0004	0.0000
500					0.0628	0.0493	0.0005
600						0.7646	0.0076
700							0.0158
800							

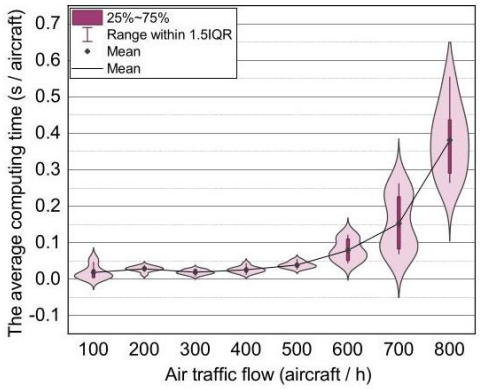

Fig. 16. Average response time.

图 16. 平均响应时间。

Table 3 shows the analysis of variance of DEP, that is P -value. It is generally believed that if P -value is less than 0.01 (bold numbers in Table 3), there is a significant statistical difference between the two groups. It was found that before the air traffic flow in the airspace was saturated, as the air traffic flow increased, the DEP did not increase significantly. There was a significant difference between the DEP when the traffic was 300 and 600 aircraft per hour, as well as 300 and 700, 400 and 600, as well as 400 and 700 aircraft per hour. This was because the DEP was too small and far less than zero when the traffic was 300 and 400 aircraft per hour, not because the DEP spiked when the traffic was 600 and 700 aircraft per hour. It was only when traffic was oversaturated, that is, at 800 aircraft per hour, that the DEP began to increase significantly.

表 3 显示了 DEP 的方差分析，即 P 值。通常认为，如果 P 值小于 0.01(表 3 中的粗体数字)，则两组之间存在显著的统计学差异。研究发现，在空域中的空中交通流量饱和之前，随着空中交通流量的增加，DEP 并没有显著增加。在交通量为每小时 300 架和 600 架飞机，以及 300 和 700、400 和 600、以及 400 和 700 架飞机之间，DEP 存在显著差异。这是因为当交通量为每小时 300 和 400 架飞机时，DEP 值太小且远小于零，并不是因为当交通量为 600 和 700 架飞机时 DEP 激增。只有当交通量过度饱和，即每小时达到 800 架飞机时，DEP 才开始显著增加。

6.2.4. Timeliness

6.2.4. 及时性

Fig. 16 shows that before the air traffic flow in the airspace was saturated, the computing time was kept below 0.1 s, which could meet the real-time operation requirements. When the flow exceeded the threshold, the computing time increased significantly, which also showed that in actual operation, the flow should be controlled and kept within the threshold.

图 16 显示，在空域中的空中交通流量饱和之前，计算时间保持在 0.1 秒以下，这可以满足实时操作要求。当流量超过阈值时，计算时间显著增加，这也表明在实际操作中，流量应当被控制并保持在阈值范围内。

Fig. 17 shows the computing time for key steps, that is, airspace parameterisation, pre-planning and real-time re-planning. Airspace parameterisation refers to the computing time required for the generating discretised airspace model. The calculations for the airspace parameterisation will be done on a ground-based computer in practice. In this case study, the computing time for the airspace parameterisation was about 5.6s. Although the airspace model (and in particular the restricted area model) was simplified in this case study, this computing time

for airspace parameterisation may even be shorter in practice, considering that the actual ground-based computers used in practice are most likely to have a much higher computational performance than the personal computers used for the experiments in this paper. Pre-planning refers to the computing time for autonomous planning of the desired trajectory. In this case study, without regard to the coordination process, the average computing time for pre-planning per aircraft was about 0.003 s. This very short period of time would be negligible even in real-time, let alone the fact that it actually occurred before entry. Real-time re-planning refers to the computing time for autonomous re-planning of optimal agreed trajectory inside the sector. The computing time for real-time re-planning shown in Fig. 17 is the average value that comes from Fig. 16. Considering that the computing time for pre-planning and real-time re-planning is very short, this computation would possibly be done on an onboard computer in practice. Besides, in the optimal solution search method (Section 5.2.5), the computation of each potential feasible point is independent of the others. Therefore, for a larger scale scenario, parallel computing would greatly reducing the computing time.

图 17 显示了关键步骤的计算时间，即空域参数化、预规划和实时重新规划。空域参数化指的是生成离散空域模型所需的计算时间。在实际操作中，空域参数化的计算将在地面计算机上完成。在本案例研究中，空域参数化的计算时间约为 5.6 秒。尽管在本案例研究中对空域模型 (尤其是限制区域模型) 进行了简化，但考虑到实际中使用的地面计算机很可能具有比本文实验中使用的个人计算机更高的计算性能，空域参数化的计算时间在实际中甚至可能更短。预规划指的是自主规划期望轨迹的计算时间。在本案例研究中，不考虑协调过程，每架飞机的预规划平均计算时间约为 0.003 秒。这个非常短的时间即使在实时情况下也可以忽略不计，更不用说它实际上发生在进入之前。实时重新规划指的是在扇区内部自主重新规划最优协商轨迹的计算时间。图 17 中显示的实时重新规划的计算时间是来自图 16 的平均值。考虑到预规划和实时重新规划的计算时间非常短，这种计算在实际中可能会在机载计算机上完成。此外，在最优解搜索方法 (第 5.2.5 节) 中，每个潜在可行点的计算都是独立的。因此，对于更大规模的场景，并行计算将大大减少计算时间。

In addition, our team's previous paper discussed sensitivity analysis, and the same conclusions were found in this simulation. Readers are encouraged to refer to the findings of the previous work (Yutong et al., 2020) for further details. The main conclusions are as follows:

此外，我们团队之前的论文讨论了敏感性分析，本次模拟也得到了相同的结论。建议读者参考之前工作 (Yutong et al., 2020) 的发现以获取更多详细信息。主要结论如下:

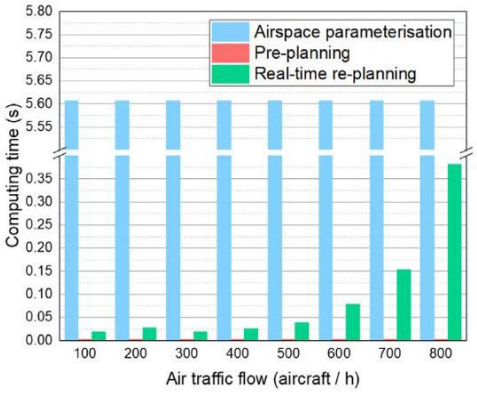

Fig. 17. Computing time for key steps.

图 17. 关键步骤的计算时间。

1. The smaller the grid size is, the better the optimisation effect will be, but the longer the required calculation time will be. 2. The higher the traffic density is, the longer the calculation time becomes.

1. 网格尺寸越小，优化效果越好，但所需的计算时间越长。2. 交通密度越高，计算时间越长。

7. Conclusions and future work

7. 结论与未来工作

In this paper, an autonomous planning method of optimal 4D trajectory for real-time en-route airspace operation is proposed to enhance the potential for practical application of conflict detection and resolution technology. A general framework of autonomous trajectory operating system is designed, including a grid-based airspace discretisation module (Module I), an initial conflict-free trajectory planning module (Module II), a trajectory pre-planning based

on the temporarily restricted area module (Module III), and a real-time conflict-free 4D trajectory planning module (Module IV). Modules III and IV form a two-stage real-time autonomous 4D trajectory planning method making this method compatible with the current trajectory-based operation mechanism. This method takes into account 3D scenarios, controlled time of arrival, restricted areas, trajectory recovery and multi-stakeholder performance preferences for practical applications. The solution space visualisation of this method provides a reference pathway for enhancing the human-machine interaction in autonomous operations.

本文提出了一种实时航路空域运行的最优 4D 轨迹自主规划方法，以增强冲突检测与解决技术在实际应用中的潜力。设计了一个自主轨迹操作系统的一般框架，包括基于网格的空域离散化模块 (模块 I)、初始无冲突轨迹规划模块 (模块 II)、基于临时限制区域的轨迹预规划模块 (模块 III) 以及实时无冲突 4D 轨迹规划模块 (模块 IV)。模块 III 和 IV 构成了一种两阶段的实时自主 4D 轨迹规划方法，使该方法与当前的基于轨迹的运行机制兼容。该方法考虑了三维场景、控制到达时间、限制区域、轨迹恢复以及多方利益相关者的性能偏好等实际应用因素。该方法的解空间可视化为进一步增强自主操作中的人机交互提供了参考路径。

The performance of the proposed method was verified by simulations. The results show the following:

通过模拟验证了所提出方法的有效性。结果显示以下内容:

1. This method can realise effective CD&R in the 3D airspace with restricted area. The maximum air traffic flow per hour in a 300 km $\times$ 300 km $\times$ 6 FL airspace with an unusable area of 60 km $\times$ 60km $\times$ 4 F was 600 aircraft per hour, which is several times that in real-world operation.

1. 该方法能够在有限制区域的 3D 空域中实现有效的冲突检测与解决。在 300 km $\times$ 300 km $\times$ 6 FL 空域中，一个不可用区域为 60 km $\times$ 60km $\times$ 4 F 的最大空中交通流量为每小时 600 架次，这是实际运行中的数倍。

2. Autonomous operation based on this method can effectively reduce the additional operating cost of the aircraft. In the case of air traffic flow saturation in the airspace, the average additional flight distance, flight delays, and fuel consumption were controlled at 0.41 km, 2.1 s, 1.5 kg , respectively.

2. 基于这种方法进行的自主运行可以有效降低飞机的额外运营成本。在空域空中交通流量饱和的情况下，平均额外飞行距离、飞行延误和燃油消耗分别控制在 0.41 km, 2.1 s, 1.5 kg 。

3. Autonomous operation based on this method can keep the domino effect at a lower level, and with the increase in the air traffic flow in the airspace, the domino effect will not increase significantly.

3. 基于这种方法的自主运行可以保持多米诺效应在较低水平，并且随着空域内空中交通流量的增加，多米诺效应不会显著增加。

4. The method has a computing speed that satisfies the real-time operation. When the airspace air traffic flow is lower than the threshold value, the average computing time efficiency of this method in the real-time operation stage was 0.1 s.

4. 该方法具有满足实时运行的计算速度。当空域内空中交通流量低于阈值时，该方法在实时运行阶段的平均计算时间效率为 0.1 秒。

In future research, we will quantitatively investigate the impact of the solution space visualisation method on human-machine interaction through human-in-the-loop experiments. The proposed operational framework will be enhanced to cope with the uncertainty and dynamics of the airspace environment and will be validated in real airspace data. Multi-aircraft trajectory negotiation based on reachable solution space is also of interest to improve the multiple optimisation objective trade-offs for autonomous trajectory operations. Additionally, research into the integration of pre-tactical (demand and capacity balancing) and tactical (conflict detection and resolution) conflict management in the concept of trajectory-based operation has the potential to facilitate the practical application of the autonomous ATM.

在未来的研究中，我们将通过人类在环实验定量研究解决方案空间可视化方法对人与人机交互的影响。提出的运行框架将得到加强，以应对空域环境的不确定性和动态性，并将在真实空域数据中得到验证。基于可达解决方案空间的多人飞机轨迹协商也是感兴趣的领域，以改善自主轨迹运行的多目标优化权衡。此外，研究在基于轨迹运行的概念中整合预先战术 (需求和容量平衡) 和战术 (冲突检测和解决) 冲突管理，有潜力促进自主空中交通管理 (ATM) 的实际应用。

CRediT authorship contribution statement

贡献声明

Yutong Chen: Methodology, Validation, Writing - original draft. Minghua Hu: Supervision, Writing - review & editing. Lei Yang: Conceptualization, Writing - original draft, Writing - review & editing.

Yutong Chen: 方法论，验证，撰写 - 原始草稿。Minghua Hu: 监督，撰写 - 审阅与编辑。Lei Yang: 概念化，撰写 - 原始草稿，撰写 - 审阅与编辑。

Acknowledgements

致谢

This article is funded by National Natural Science Foundation of China (No. 61903187), Natural Science Foundation of Jiangsu Province, China (BK20190414), Postgraduate Research Innovation Program of Jiangsu, China (KYCX20_0213), and Interdisciplinary Innovation Foundation for Postgraduates of NUAA, China (KXKCXJJ202001), China Scholarship Council (No. 202006830095).

本文得到国家自然科学基金 (编号:61903187)、江苏省自然科学基金 (BK20190414)、江苏省研究生科研创新计划 (KYCX20_0213) 以及南京航空航天大学研究生跨学科创新基金 (KXKCXJJ202001)、中国留学基金委 (编号:202006830095) 的资助。

References

参考文献

Alam, S., Shafi, K., Abbass, H.A., Barlow, M., 2009. An ensemble approach for conflict detection in free flight by data mining. Transp. Res. C 17 (3), 298-317.

Alonso-Ayuso, A., Escudero, L.F., Martín-Campo, F.J., 2010. Collision avoidance in air traffic management: A mixed-integer linear optimization approach. IEEE

Alonso-Ayuso, A., Escudero, L.F., Martín-Campo, F.J., 2016. Multiobjective optimization for aircraft conflict resolution. a metaheuristic approach. European J. Oper. Res. 248 (2), 691-702.

Alonso-Ayuso, A., Escudero, L.F., Martin-Campo, F.J., Mladenović, N., 2017. On the aircraft conflict resolution problem: A VNS approach in a multiobjective framework. Electron. Notes Discrete Math. 58, 151-158.

Bilimoria, K., Sheth, K., Lee, H., Grabbe, S., 2000. Performance evaluation of airborne separation assurance for free flight. In: 18th Applied Aerodynamics Conference. p. 4269.

Blom, H.A., Bakker, G., 2016. Agent-based modelling and simulation of trajectory based operations under very high traffic demand. In: Proc. SESAR innovation days.

Calvo-Fernández, E., Perez-Sanz, L., Cordero-García, J.M., Arnaldo-Valdés, R.M., 2017. Conflict-free trajectory planning based on a data-driven conflict-resolution model. J. Guid. Control Dyn. 40 (3), 615-627.

Cecen, R.K., Cetek, C., 2019. A two-step approach for airborne delay minimization using pretactical conflict resolution in free-route airspace. J. Adv. Transp. 2019.

Cobano, J.A., Alejo, D., Heredia, G., Ollero, A., 2013. 4D trajectory planning in ATM with an anytime stochastic approach. In: Proceedings of the 3rd International Conference on Application and Theory of Automation in Command and Control Systems. pp. 1-8.

Coletsos, J., Ntakolia, C., 2017. Air traffic management and energy efficiency: the free flight concept. Energy Syst. 8 (4), 709-726.

Dijkstra, E.W., et al., 1959. A note on two problems in connexion with graphs. Numer. Math. 1 (1), 269-271.

Djokic, J., Lorenz, B., Fricke, H., 2010. Air traffic control complexity as workload driver. Transp. Res. C 18 (6), 930-936.

Dong, S., Weiping, X., Zhang, K., 2022. Study on the resolution of multi-aircraft flight conflicts based on an IDQN. Chin. J. Aeronaut. 35 (2), 195-213.

Drupka, G., Majka, A., Rogalski, T., Trela, L., 2018. An airspace model aplicable for automatic flight route planning inside free route airspace. Zeszyty Naukowe Politechniki Rzeszowskiej. Mechanika.

Edwards, T., Homola, J., Mercer, J., Claudatos, L., 2017. Multifactor interactions and the air traffic controller: the interaction of situation awareness and workload in association with automation. Cogn. Technol. Work 19 (4), 687-698.

EUROCONTROL, 2010. User manual for the base of aircraft data (BADA) revision 3.8. Brussels, https://www.eurocontrol.int/pu manual-base-aircraft-data-bada-revision-38.

EUROCONTROL, 2020. All-causes delay and cancellations to air transport in Europe for 2019. Brussels, https://www.eurocontrol.int/sites/default/files/2020- 04/eurocontrol-coda-digest-annual-report-2019.pdf.

Eyferth, K., Niessen, C., Spaeth, O., 2003. A model of air traffic controllers' conflict detection and conflict resolution. Aerosp. Sci. Technol. 7 (6), 409-416.

Gardi, A., Sabatini, R., Kistan, T., Lim, Y., Ramasamy, S., 2015. 4 dimensional trajectory functionalities for air traffic management systems. In: 2015 integrated communication, navigation and surveillance conference. ICNS, IEEE, pp. N3-1.

Gaxiola, C.A.N., Barrado, C., Royo, P., Pastor, E., 2018. Assessment of the north European free route airspace deployment. J. Air Transp. Manag. 73, 113-119. Han, Y.-X., Zhang, J.-W., Huang, X.-Q., 2019. Method for optimal conflict-free aircraft trajectory generation. Aircr. Eng. Aerosp. Technol.

Hoekstra, J.M., van Gent, R.N., Ruigrok, R.C., 2002. Designing for safety: the 'free flight'air traffic management concept. Reliab. Eng. Syst. Saf. 75 (2), 215-232. Hoekstra, J., Ruigrok, R., Van Gent, R., 2001. Free flight in a crowded airspace? Progr. Astronaut. Aeronaut. 193, 533-546.

Hu, X.-B., Wu, S.-F., Jiang, J., 2004. On-line free-flight path optimization based on improved genetic algorithms. Eng. Appl. Artif. Intell. 17 (8), 897-907.

ICAO, 2005. Global air traffic management operational concept. Montréal, https://www.icao.int/Meetings/anconf12/Document%
pdf.ICAO, 2013. 2013-2028 Global air navigation plan. Montréal, https://www.icao.int/publications/Documents/9750_4ed_en.pdf.

Idris, H., Enea, G., Lewis, T.A., 2016. Function allocation between automation and human pilot for airborne separation assurance. IFAC-PapersOnLine 49 (19), 25-30.

Kahne, S., 2000. Research issues in the transition to free flight. Annu. Rev. Control 24, 21-29.

Kaluder, H., Brezak, M., Petrović, I., 2011. A visibility graph based method for path planning in dynamic environments. In: 2011 Proceedings of the 34th International Convention MIPRO. IEEE, pp. 717-721.

Karikawa, D., Aoyama, H., 2016. Analysis of controllers' working methods supporting safe and efficient air traffic operations. IFAC-PapersOnLine 49 (19), 319-324.

Klomp, R., Borst, C., van Paassen, R., Mulder, M., 2015. Expertise level, control strategies, and robustness in future air traffic control decision aiding. IEEE Trans. Hum.-Mach. Syst. 46 (2), 255-266.

lomp, R., Riegman, R., Borst, C., Mulder, M., Van Paassen, M., 2019. Solution space concept: human-machine interface for 4D trajectory management. In: Proc. of the Thirteenth USA/Europe Air Traffic Management Research and Development Seminar. ATM2019, (58), pp. 17-21.

Kreuz, M., Luchkova, T., Schultz, M., 2016. Effect of restricted airspace on the ATM system. In: WCTR conference.

Kupfer, M., Farley, T., Chu, Y., Erzberger, H., 2008. Automated conflict resolution-a simulation-based sensitivity study of airspace and demand. In: Proc 26th International Congress of the Aeronautical Sciences.

Lai, H.-Y., Chen, C.-H., Khoo, L.-P., Zheng, P., 2019. Unstable approach in aviation: Mental model disconnects between pilots and air traffic controllers and interaction conflicts. Reliab. Eng. Syst. Saf. 185, 383-391.

Landry, S.J., Lagu, A., Kinnari, J., 2010. State-based modeling of continuous human-integrated systems: An application to air traffic separation assurance. Reliab. Eng. Syst. Saf. 95 (4), 345-353.

Lozano-Pérez, T., Wesley, M.A., 1979. An algorithm for planning collision-free paths among polyhedral obstacles. Commun. ACM 22 (10), 560-570.

Malaek, S.M.-B., Golchoubian, M., 2020. Enhanced conflict resolution maneuvers for dense airspaces. IEEE Trans. Aerosp. Electron. Syst. 56 (5), 3409-3420.

Marshall, C., Roberts, B., Grenn, M., 2017. Intelligent control & supervision for autonomous system resilience in uncertain worlds. In: 2017 3rd international conference on control, automation and robotics. ICCAR, IEEE, pp. 438-443.

Miller, H.J., 1991. Modelling accessibility using space-time prism concepts within geographical information systems. Int. J. Geogr. Inf. Syst. 5 (3), 287-301. Omer, J., 2015. A space-discretized mixed-integer linear model for air-conflict resolution with speed and heading maneuvers. Comput. Oper. Res. 58, 75-86.

Pappas, G., Tomlin, C., Lygeros, J., Godbole, D., Sastry, S., 1997. A next generation architecture for air traffic management systems. In: Proceedings of the 36th IEEE conference on decision and control, Vol.3. IEEE, pp. 2405-2410.

Pritchett, A.R., Genton, A., 2017. Negotiated decentralized aircraft conflict resolution. IEEE Trans. Intell. Transp. Syst. 19 (1), 81-91.

Rezo, Z., Steiner, S., 2020. South east common Sky initiative free route airspace-implementation aftermath. Transp. Res. Proc. 45, 676-683.

Ruigrok, R.C., Hoekstra, J.M., 2007. Human factors evaluations of free flight: Issues solved and issues remaining. Applied Ergon. 38 (4), 437-455.

luiz, S., Piera, M.A., Nosedal, J., Ranieri, A., 2014. Strategic de-confliction in the presence of a large number of 4D trajectories using a causal modeling approach. Transp. Res. C 39, 129-147.

Saez Nieto, F.J., 2016. The long journey toward a higher level of automation in ATM as safety critical, sociotechnical and multi-agent system. Proc. Inst. Mech.

Eng. G 230 (9), 1533-1547.

Eng. G 230 (9), 1533-1547。

Seah, C.E., Hwang, L., 2009. Stochastic linear hybrid systems: Modeling, estimation, and application in air traffic control. IEEE Trans. Control Syst. Technol. 17 (3), 563-575.

Seenivasan, D.B., Olivares, A., Staffetti, E., 2020. Multi-aircraft optimal 4D online trajectory planning in the presence of a multi-cell storm in development. Transp. Res. C 110, 123-142.

Shijin, W., Xi, C., Haiyun, L., Qingyun, L., Xu, H., Yanjun, W., 2017. Air route network optimization in fragmented airspace based on cellular automata. Chin. J. Aeronaut. 30 (3), 1184-1195.

Šišlák, D., Volf, P., Pěchouček, M., 2010. Agent-based cooperative decentralized airplane-collision avoidance. IEEE Trans. Intell. Transp. Syst. 12 (1), 36-46. Strybel, T.Z., Chiappe, D., Vu, K.-P.L., Miramontes, A., Battiste, H., Battiste, V., 2016. A comparison of methods for assessing situation awareness in current day and future air traffic management operations: Graphics-based vs text-based online probe systems. IFAC-PapersOnLine 49 (19), 31-35.

Sun, M., Rand, K., Fleming, C., 2019. 4 dimensional waypoint generation for conflict-free trajectory based operation. Aerosp. Sci. Technol. 88, 350-361.

Velasco, G.M., Mulder, M., van Paassen, M.M., 2010. Air traffic controller decision-making support using the solution space diagram. IFAC Proc. Vol. 43 (13), 227-232.

Walter, L., Kostina, E., 2014. Optimal control framework for a centralized approach to separation management. J. Guid. Control Dyn. 37 (3), 1033−1038.

Wang, R., Alligier, R., Allignol, C., Barnier, N., Durand, N., Gondran, A., 2020. Cooperation of combinatorial solvers for en-route conflict resolution. Transp. Res. C 114, 36-58.

Weitz, L.A., Sgorcea, R., Boyd, A., 2019. Designing instrument approach procedures compatible with the use of ATC automation for trajectory-based operations. In: AIAA Scitech 2019 Forum. p. 0434.

Westin, C., Borst, C., Hilburn, B., 2016. Automation transparency and personalized decision support: Air traffic controller interaction with a resolution advisory

Wu, S., Liu, X., 1994. Optimized sequencing and scheduling algorithms for arrival air traffics based on FCFS principles. IFAC Proc. Vol. 27 (12), 215-218.

Xu, Y., Dalmau, R., Melgosa, M., Montlaur, A., Prats, X., 2020. A framework for collaborative air traffic flow management minimizing costs for airspace users: Enabling trajectory options and flexible pre-tactical delay management. Transp. Res. B 134, 229-255.

Yutong, C., Minghua, H., Lei, Y., Haoran, Z., Zheng, Z., 2020. Autonomous trajectory planning and conflict management technology in restricted airspace. Acta Aeronaut. Astronaut. Sinica 41 (09), 253-270.

Zhu, C., Wu, J., Liu, M., Wang, L., Li, D., Kouvelas, A., 2021. Recovery preparedness of global air transport influenced by COVID-19 pandemic: Policy intervention analysis. Transp. Policy 106, 54-63.